Synthesis and Photoexcited-State Dynamics of Aromatic Group-Bridged Carotenoid–Porphyrin Dyads and Carotenoid–Porphyrin–Pyromellitimide Triads

Atsuhiro Osuka,*[1a] Hiroko Yamada,[1a] Kazuhiro Maruyama,[1a] Noboru Mataga,*[1b] Tsuyoshi Asahi,[1b] Masaya Ohkouchi,[1b] Tadashi Okada,[1b] Iwao Yamazaki,[1c] and Yoshinobu Nishimura[1c]

Contribution from the Department of Chemistry, Faculty of Science, Kyoto University, Kyoto 606, Japan, Department of Chemistry, Faculty of Engineering Science, Osaka University, Toyonaka 560, Japan, and Department of Chemical Process Engineering, Faculty of Engineering, Hokkaido University, Sapporo 060, Japan

*Received February 1, 1993**

Abstract: A series of conformationally restricted carotenoid–porphyrin dyads (C–H_2P and C–ZnP) was prepared by trichloroacetic acid-catalyzed condensation of a carotenoid-substituted aromatic aldehyde and 4-(methoxycarbonyl)-benzaldehyde with bis(3-hexyl-4-methyl-2-pyrrolyl)methane in a benzene–acetonitrile mixture. Spacers between the carotenoid and the porphyrin cover aromatic groups including benzene, naphthalene, biphenyl, diphenylmethane, spirobiindane, and benzanilide. Carotenoid–porphyrin–pyromellitimide triads (C–H_2P–Im) were similarly prepared using *N*-hexyl-*N'*-(4-formylphenyl)methyl)pyromellitimide instead of 4-(methoxycarbonyl)benzaldehyde. Photoexcited-state dynamics of these models were studied by steady-state fluorescence spectra, fluorescence excitation spectra, picosecond time-resolved fluorescence lifetime measurements, and picosecond time-resolved transient absorption spectroscopy. Intramolecular singlet–singlet energy transfer in C–H_2P has been revealed to be a reversible process, while only one-way singlet–singlet energy transfer from zinc porphyrin to carotenoid has been observed in C–ZnP. Rates of the intramolecular energy transfer ^{1}(C)*–H_2P → C–^{1}(H_2P)* were determined from efficiencies of the energy transfer that were obtained by comparing their fluorescence excitation spectra with the absorption spectra, and rates of C–^{1}(H_2P)* → ^{1}(C)*–H_2P and of C–^{1}(ZnP)* → ^{1}(C)*–ZnP were determined on the basis of their fluorescence lifetimes. The rates of the intramolecular energy transfer depend on the spacer between C and P in a rather similar manner through these three different energy-transfer processes and are quite sensitive to the substitution position of the aromatic spacer where the porphyrin is linked to the carotenoid. These spacer dependencies observed indicate the through-bond electronic coupling to be the most important interactions in these intramolecular energy transfers. In C–H_2P–Im triads, excitation at C with 532-nm light led to an accumulation of (C)$^+$–H_2P–(Im)$^-$ within several tens of picoseconds. This rapid accumulation had been interpreted in terms of long-distance electron transfer from ^{1}(C)* to Im mediated by a superexchange interaction involving the π-electronic orbital of the intervening H_2P. Selective excitation of the triad to C–^{1}(H_2P)*–Im at 585 nm led to much slower formation of (C)$^+$–H_2P–(Im)$^-$, probably via a ^{1}(C)*–H_2P–Im state which may be formed by intramolecular singlet–singlet energy transfer.

Introduction

Carotenoids are ubiquitous in photosynthetic organisms and essential for their survival. They have two important functions in photosynthetic organisms: they serve as accessory light-harvesting pigments transferring their excitation energy to chlorophyll, where it can be used for photosynthetic work,[2-5] and they also protected the photosynthetic apparatus from harmful photooxidation reactions.[6-13] Both these functions, light harvesting as well as photoprotection, involve excitation energy transfer: single–singlet from carotenoid to chlorophyll and triplet–triplet from chlorophyll to carotenoid, respectively.

These energy-transfer reactions were demonstrated in artificial, covalently linked carotenoid–porphyrin dyads. In 1980, Gust and Moore prepared ester-linked carotenoid–tetraarylporphyrin dyads and observed for the first time an efficient intramolecular singlet–singlet energy transfer (EN) from carotenoid to porphyrin in a stacked model.[14] But in an analgous molecule with an extended conformation, they did not observe such EN. On the basis of these results, they suggested the importance of a stacked conformation for efficient EN. Using the same models, they confirmed the photoprotection function also by monitoring diphenylbenzofuran photooxidation as well as by tracing the formation and decay of the triplet excited states of carotenoid and porphyrins.[15] Singlet–singlet EN from the carotenoid to the porphyrin and triplet–triplet EN from the porphyrin to the carotenoid were observed in other models.[16-20]

* Abstract published in *Advance ACS Abstracts*, September 15, 1993.

(1) (a) Kyoto University. (b) Osaka University. (c) Hokkaido University.

(2) Cogdell, R. J.; Hipkins, M. F.; MacDonald, W.; Truscott, T. G. *Biochim. Biophys. Acta* **1981**, *634*, 191.

(3) Goedheer, J. C. *Biochim. Biophys. Acta* **1959**, *35*, 1.

(4) Siefermann-Harms, D. *Biochim. Biophys. Acta* **1985**, *811*, 325.

(5) van Grondelle, R.; Kramer, H. J. M.; Rijigersberg, C. P. *Biochim. Biophys. Acta* **1982**, *682*, 208.

(6) Griffiths, M.; Sistrom, W. R.; Cohen-Bazire, G.; Stanier, R. Y. *Nature* **1955**, *176*, 1211.

(7) Cohen-Bazire, G.; Stanier, R. Y. *Nature* **1958**, *181*, 250.

(8) Krinsky, N. I. *Pure Appl. Chem.* **1979**, *51*, 649.

(9) (a) Chadwick, B. W.; Frank, H. A. *Biochim. Biophys. Acta* **1986**, *851*, 257. (b) Frank, H. A.; Violette, C. A. *Biochim. Biophys. Acta* **1989**, *976*, 222.

(10) Mathis, P., Butler, W. L.; Satoh, K. *Photochem. Photobiol.* **1979**, *30*, 603.

(11) Foote, C. S.; Denny, R. W. *J. Am. Chem. Soc.* **1968**, *90*, 6233.

(12) Davidson, E.; Cogdell, R. J. *Biochim. Biophys. Acta* **1981**, *635*, 295.

(13) Monger, T. G.; Cogdell, R. I.; Parson, W. W. *Biochim. Biophys. Acta* **1976**, *449*, 139.

(14) (a) Dirks, G.; Moore, A. L.; Moore, T. A.; Gust, D. *Photochem. Photobiol.* **1980**, *32*, 277. (b) Moore, A. L.; Dirks, G.; Gust, D.; Moore, T. A. *Photochem. Photobiol.* **1980**, *32*, 691.

(15) Bensasson, R. V.; Land, E. J.; Moore, A. L.; Crouch, R. L.; Dirks, G.; Moore, T. A.; Gust, D. *Nature* **1981**, *290*, 329.

(16) Liddell, P. A.; Nemeth, G. A.; Lehman, W. R.; Joy, A. M.; Moore, A. L.; Bensasson, R. V.; Moore, T. A.; Gust, D. *Photochem. Photobiol.* **1982**, *36*, 641.

0002-7863/93/1515-9439$04.00/0

Chart I. Structures of Carotenoid–Porphyrin (C–P) Dyads Studied in This Paper[a]

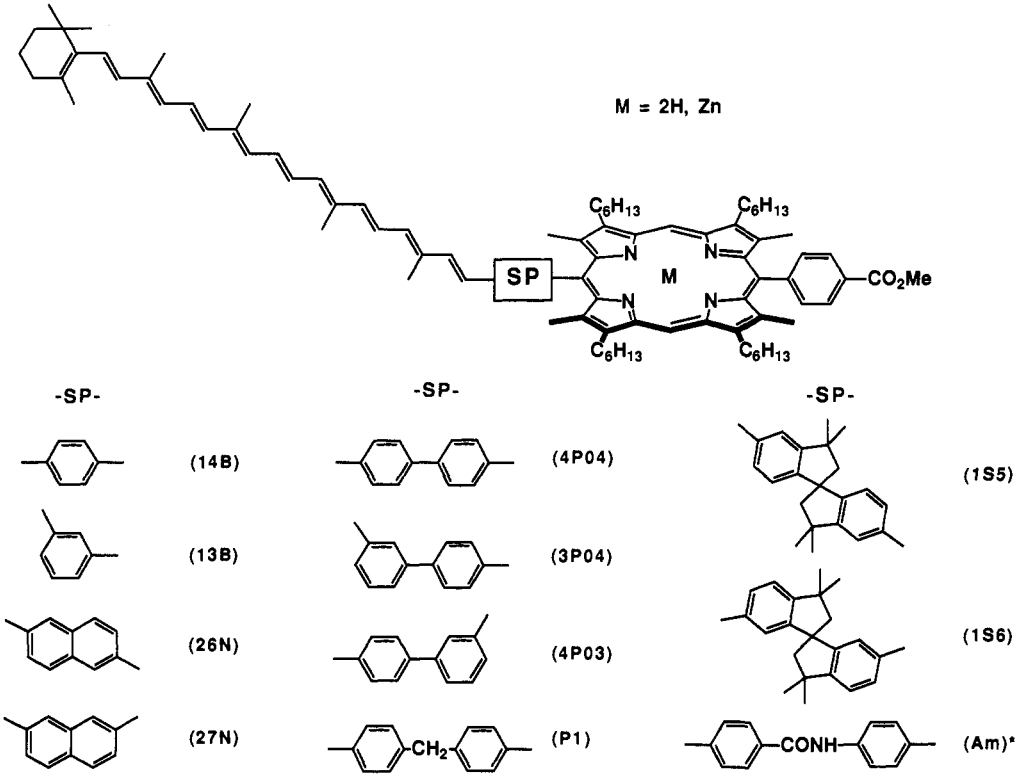

[a] Abbreviations are indicated in parentheses at the right side of the aromatic spacers. In an Am-bridged molecule, the 4-methoxycarbonyl group was replaced by a methyl group.

In addition to the two key biomimetic functions noted above, two photochemical reactions have been unmasked through studies on their model compounds: (1) first excited singlet states of porphyrins, in most cases free base TPP-type porphyrins, are quenched by nearby carotenoids and (2) in carotenoid–porphyrin–quinone triads and related supramolecular arrays, a photodriven multistep electron-transfer reaction generates a long-lived charge-separated state (carotenoid)$^+$–porphyrin–(quinone)$^-$. Although carotenoids have been frequently observed to quench the first excited state of nearby porphyrins and chlorophylls, the mechanisms seem to remain obscure. The fluorescence quenching by carotenoids may be related to the carotenoid-associated energy dissipation process during exposure to an excess of light in the chlorophyll pigment bed *in vivo*.[21] On the other hand, the latter functional aspect of the carotenoid, as an effective electron donor to a porphyrin cation radical, has attracted much attention in view of its utility in achieving long-lived charge-separated states.[22-24] It has been proposed that such charge-separated states are formed by a series of short-range, fast, efficient electron-transfer steps triggered by an intramolecular charge separation between the singlet excited states of the porphyrins and the quinone. Understanding the mechanisms of these photoexcited-state dynamics and the interactions of carotenoids with photosynthetic pigments will clearly help explain the biological functions of carotenoids in photosynthesis. Apparently transient absorption experiments on the picosecond or subpicosecond time scale are one of most powerful methods in elucidation of the mechanism of these photochemical events. However, systematic transient absorption studies on carotenoid-linked porphyrins have been limited so far.[20,25b,28c]

We report here the synthesis and excited-state dynamics of carotenoid–porphyrin (C–P) dyads and carotenoid–porphyrin–pyrromellitimide (C–P–Im) triads.[25] Structures of models used are summarized in Charts I and II. Our improved conditions[26] for the porphyrin cyclization method allowed the synthesis of these models directly from appropriate aromatic aldehydes and bis(3-hexyl-4-methyl-2-pyrrolyl)methane (**1**).[25a] In our models, the carotenoid (C) and porphyrin (H_2P or ZnP) are connected

(17) (a) Moore, A. L.; Joy, A.; Tom, R.; Gust, D.; Moore, T. A.; Bensasson, R. V.; Land, E. J. *Science* **1982**, *216*, 982. (b) Gust, D.; Moore, T. A.; Bensasson, R. V.; Mathis, P.; Land, E. J.; Chachaty, C.; Moore, A. L.; Liddell, P. A.; Nemeth, G. A. *J. Am. Chem. Soc.* **1985**, *107*, 3631.

(18) Gust, D.; Moore, T. A.; Moore. A. L.; Devadoss, C.; Liddell, P. A.; Hermant, R.; Nieman, R. A.; Demanche, L. J.; DeGraziano, J. M.; Gouni, I. *J. Am. Chem. Soc.* **1992**, *114*, 3950.

(19) Gust, D.; Moore, T. A.; Moore, A. L.; Gao, F.; Luttrull, D.; DeGraziano, J. M.; Ma, X. C.; Makings, L. R.; Lee, S.-J.; Trier, T. T.; Bittersmann, E.; Seely, G. R.; Woodward, S.; Bensasson, R. V.; Rougee, M.; De Schryver, F. C.; Van der Auweraer, M. *J. Am. Chem. Soc.* **1991**, *113*, 3638.

(20) Wasielewski, M. R.; Liddell, P. A.; Barrett, D.; Moore, T. A.; Gust, D. *Nature* **1986**, *322*, 570.

(21) Demmig-Adams, B. *Biochim. Biophys. Acta* **1990**, 1020, 1.

(22) (a) Gust, D.; Moore, T. A. *J. Photochem.* **1985**, *29*, 173. (b) Gust, D.; Moore, T. A. *Science* **1989**, *244*, 35.

(23) (a) Moore, T. A.; Gust, D.; Mathis, P.; Mialocq, J.-C.; Chachaty, C.; Bensasson, R. V.; Land, E. J.; Doizi, D.; Liddell, P. A.; Lehman, W. R.; Nemeth, G. A.; Moore, A. L. *Nature* **1984**, *307*, 630. (b) Seta, P.; Bienvenue, E.; Moore, A. L.; Mathis, P.; Bensasson, R. V.; Liddell, P.; Pessiki, P. J.; Joy, A.; Moore, T. A.; Gust, D. *Nature* **1985**, *316*, 653. (c) Liddell, P. A.; Barrett, D.; Makings, L. R.; Pessiki, P. J.; Gust, D.; Moore, T. A. *J. Am. Chem. Soc.* **1986**, *108*, 5350. (d) Gust, D.; Moore, T. A.; Makings, L. R.; Liddell, P. A.; Nemeth, G. A.; Moore, A. L. *J. Am. Chem. Soc.* **1986**, *108*, 8028. (e) Gust, D.; Moore, T. A.; Liddell, P. A.; Nemeth, G. A.; Makings, L. R.; Moore, A. L.; Barrett, D.; Pessiki, P. J.; Bensasson, R. V.; Rougée, M.; Chachaty, C.; De Schryver, F. C.; van der Auweraer, M.; Holzwarth, A. R.; Connolly, J. S. *J. Am. Chem. Soc.* **1987**, *109*, 846. (f) Gust, D.; Moore, T. A.; Moore, A. L.; Barrett, D.; Harding, L. O.; Makings, L. R.; Liddell, P. A.; De Schryver, F. C.; van der Auweraer, M.; Bensasson, R. V.; Rougée, M. *J. Am. Chem. Soc.* **1988**, *110*, 321. (g) Gust, D.; Moore, T. A.; Moore, A. L.; Makings, L. R.; Seely, G. R.; Ma, X.; Trier, T. T.; Gao, F. *J. Am. Chem. Soc.* **1988**, *110*, 7567. (h) Gust, D.; Moore, T. A.; Moore, A. L.; Seely, G.; Liddell, P.; Barrett, D.; Harding, L. O.; Ma, X. C.; Lee, S.-J.; Gao, F. *Tetrahedron* **1989**, *45*, 4867. (i) Gust, D.; Moore, T. A.; Moore, A. L.; Lee, S.-J.; Bittersmann, E.; Luttrull, D. K.; Rehms, A. A.; DeGraziano, J. M.; Ma, X. C.; Gao, F.; Belford, R. E.; Trier, T. T. *Science* **1990**, *248*, 199. (j) Hasharoni, K.; Levanon, H.; Tang, J.; Bowman, M. K.; Norris, J. R.; Gust, D.; Moore, T. A.; Moore, A. L. *J. Am. Chem. Soc.* **1990**, *112*, 6477.

(24) Momenteau, M.; Loock, B.; Seta, P.; Bienvenue, E.; d'Epenoux, B. *Tetrahedron* **1989**, *45*, 4893.

(25) Preliminary work of this work, see: (A) Osuka, A.; Yamada, H.; Maruyama, K. *Chem. Lett.* **1990**, 1905. (b) Osuka, A.; Yamada, H.; Maruyama, K.; Mataga, N.; Asahi, T.; Yamazaki, I.; Nishimura, Y. *Chem. Phys. Lett.* **1991**, *181*, 419.

(26) (a) Nagata, T.; Osuka, A.; Maruyama, K. *J. Am. Chem. Soc.* **1990**, *112*, 3054. (b) Osuka, A.; Nagata, T.; Kobayashi, F.; Maruyama, K. *J. Heterocycl. Chem.* **1990**, *27*, 1657.

Chart II. Structures of Carotenoid–Porphyrin–Pyromellitimide Triads (C–H_2P–Im)[a]

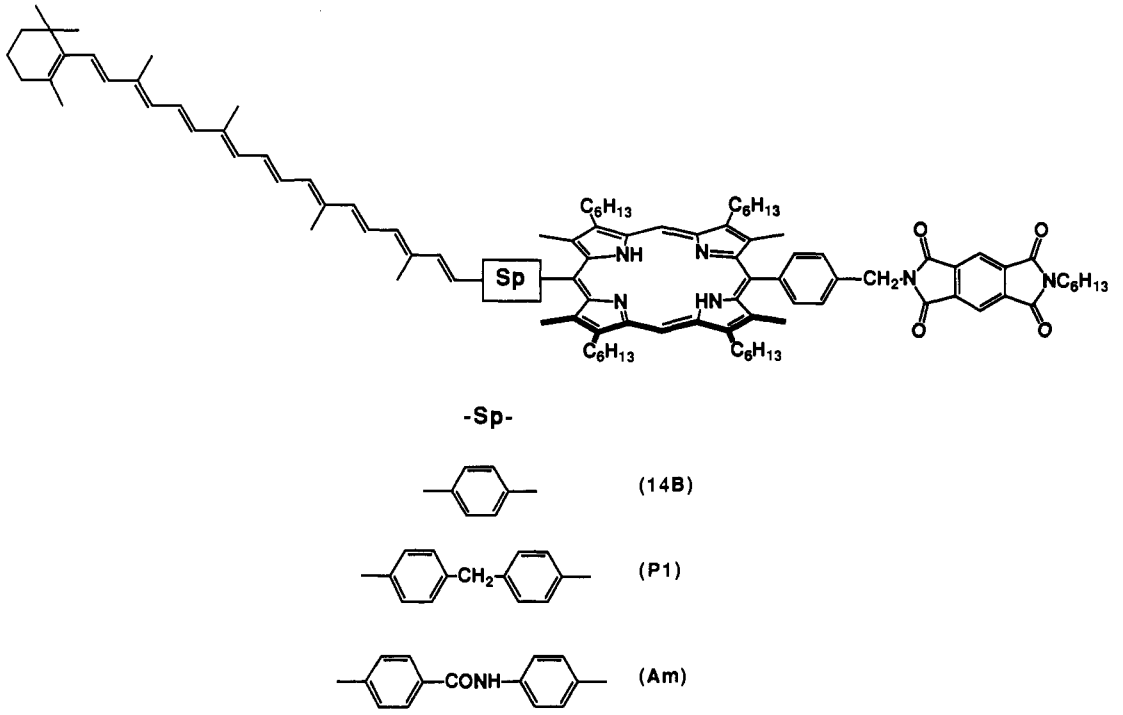

[a] Abbreviations are indicated in parentheses at the right side of the aromatic spacers.

via aromatic groups including benzene, naphthalene, biphenyl, diphenylmethane, spirobiindane, and benzanilide. We will abbreviate the names of our model molecules such as C–H_2P-(14B), indicating the species of each entity as well as a spacer between the carotenoid and porphyrin in parentheses. Abbreviations of the spacers are indicated in Charts I and II.

Due to steric repulsion between the meso-aryl bridge and the flanking methyl group, it is pertinent to assume that the aryl bridge is held at a nearly perpendicular orientation to the porphyrin plane, and that the center-to-center distances are fixed in most of the models. These conformational constraints offer the advantage that one can easily relate rates of photoexcited-state dynamics with its geometrical parameters.[27] It is also an important feature of our models that the π-electronic system of C is conjugated with aromatic spacers, and thus, in cases with such a bridge as benzene, naphthalene, or biphenyl spacers, the whole π-electronic system of an aromatic spacer-conjugated C is directly attached to the porphyrin ring with a somewhat orthogonal geometry.[28] This, naturally, causes substantial through-bond electronic interactions in these models, while such π-conjugation is interupted in models bridged by diphenylmethane or spirobiindane and is partially retained in a model bridged by a benzanilide group.

In triad models, we employed pyromellitimide (Im) as an electron acceptor, since it is an effective electron acceptor toward the singlet excited state of porphyrin[29a] and has proved to be quite useful for analysis of electron-transfer (ET) kinetics because of the characteristic sharp absorption at ca. 715 nm due to $(Im)^{-\cdot}$.[29b-d] We describe here ultrafast dynamics of C–H_2P,C–ZnP, and C–H_2P–Im revealed by picosecond time-resolved transient absorption spectroscopy. These measurements have allowed us to unveil the following new aspects of photoexcited-state dynamics in carotenoid-linked porphyrin models: (1) intramolecular singlet–singlet energy transfer from $^1(H_2P)^*$ or $^1(ZnP)^*$ to C and (2) an efficient long-distance electron transfer from $^1(C)^*$ to Im across H_2P in C–H_2P–Im.

Results

Synthesis. Carotenoid–porphyrin (C–P) dyads were prepared by trichloroacetic acid-catalyzed condensation of a carotenoid-substituted aromatic aldehyde and 4-(methoxycarbonyl)benzaldehyde (**2**) with **1** in a benzene–acetonitrile mixture (Scheme I).[25a,26b] In spite of the serious lability of carotenoids under acidic conditions, this synthetic procedure gave carotenoid-linked porphyrins in acceptable yields. At first we used *p*-tolualdehyde instead of **2**, but it was meanwhile found that separation of cross-coupled products could be performed much easier for ester-bearing molecules. The reaction shown in Scheme I produced a mixture of three porphyrins. After metallation with $Zn(OAc)_2$, a cross-condensation product was separated quickly by flash column chromatography on silica gel. Both free base forms (C–H_2P) and zinc complexes (C–ZnP) were characterized by optical and ^{1}H-NMR spectroscopy, as well as mass spectroscopy.

Precursor carotenoid-substituted aromatic aldehydes were made by Wittig reaction of the corresponding benzylphosphonium salt and 8′-apo-β-carotenal (**4**) by modification of literature methods.[24] Scheme II illustrates the synthesis of 7′-apo-7′-(4-formylphenyl)-β-carotene (**7**) from benzyl bromide **5** through phosphonium salt **6**. In all cases synthesized, the stereochemistry of a newly formed double bond was confirmed to be exclusively *trans* by large coupling constants (>14 Hz) between the $H_{7'}$ and $H_{8'}$ protons. Since the synthetic transformations involved are straightforward, details of this chemistry are not given in the

(27) This advantage has been used for a number of photosynthetic models. For reviews, see: (a) Wasielewski, M. R. *Photochem. Photobiol.* **1988**, *47*, 923. (b) Wasielewski, M. R. In *Photoinduced Electron Transfer, Part A*; Fox, M. A., Chanon, M., Eds.; Elsevier: Amsterdam, 1988; p 161. (c) Wasielewski, M. R. *Chem. Rev.* **1992**, *92*, 435. (d) Maruyama, K.; Osuka A. *Pure Appl. Chem.* **1990**, *62*, 1511.

(28) Similar polyene-linked porphyrins with direct attachment were reported, see: (a) Effenberger, F.; Schlosser, H.; Bäuerle, P.; Maiser, S.; Port, H.; Wolf, H. C. *Angew. Chem., Int. Ed. Engl.* **1988**, *27*, 281. (b) Effenberger, F.; Schlosser, H. *Synthesis* **1990**, 281. (c) Wasielewski, M. R.; Johnson, D. G.; Svec, W. A.; Kersey, K. M.; Cragg, D. E.; Minsek, D. W. In *Photochemical Energy Conversion*; Norris, J. R., Meisel, D., Eds.; Elsevier: Amsterdam, 1989; pp 135.

(29) (a) Cowan, J. A.; Sanders, J. K. M. *J. Chem. Soc., Perkin Trans. 1* **1985**, 2435. (b) Osuka, A.; Nakajima, S.; Maruyama, K.; Mataga, N.; Asahi, T. *Chem. Lett.* **1991**, 1003. (c) Osuka, A.; Nagata, T.; Maruyama, K.; Mataga, N.; Asahi, T.; Yamazaki, I.; Nishimura, Y. *Chem. Phys. Lett.* **1991**, *185*, 88. (d) Osuka, A.; Nagata, T.; Kobayashi, F.; Zhang, R. P.; Maruyama, K.; Mataga, N.; Asahi, T.; Ohno, K.; Nozaki, K. *Chem. Phys. Lett.* **1992**, *199*, 302.

Scheme I. Synthesis of Dyads (C–P) and Triads (C–P–Im)[a]

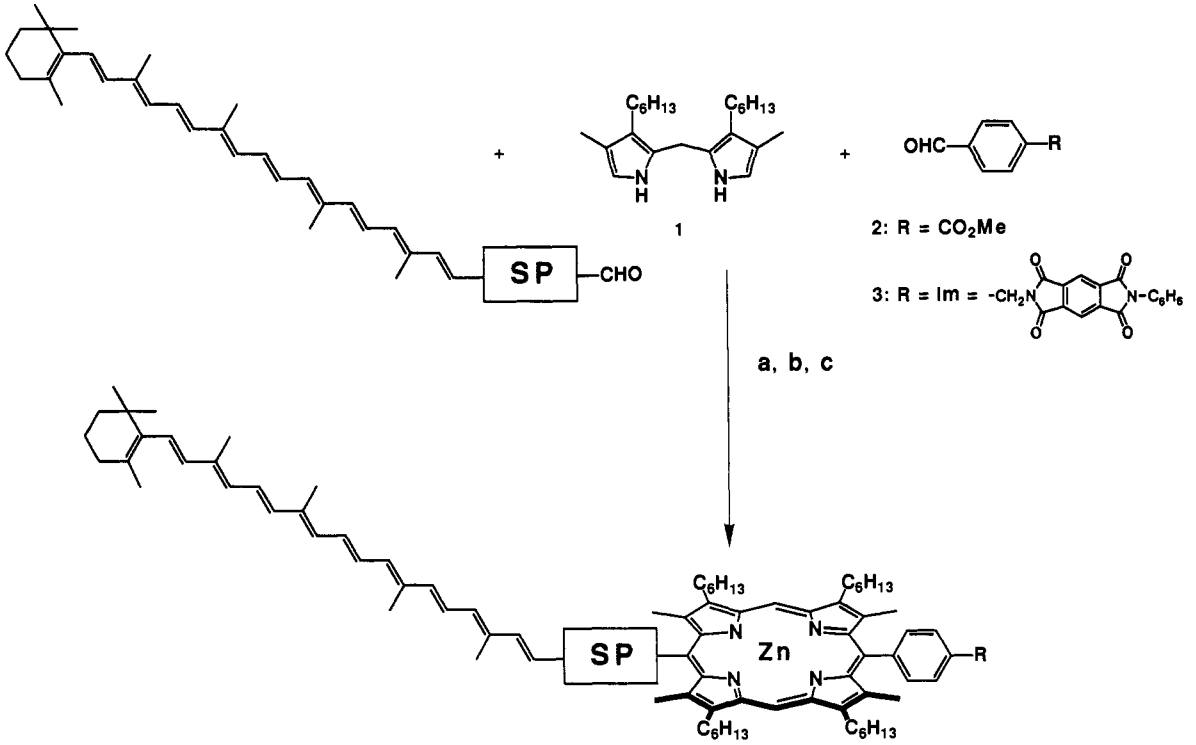

[a] (a) CCl_3CO_2H, CH_3CN–C_6H_6 (7/3), room temperature 8 h, (b) chloranil, THF, room temperature, 2 h, (c) $Zn(OAc)_2$, MeOH, room temperature, 10 min.

Scheme II. Synthesis of Carotenoid–Substituted Aromatic Aldehyde **7** from Benzyl Bromide **5**[a]

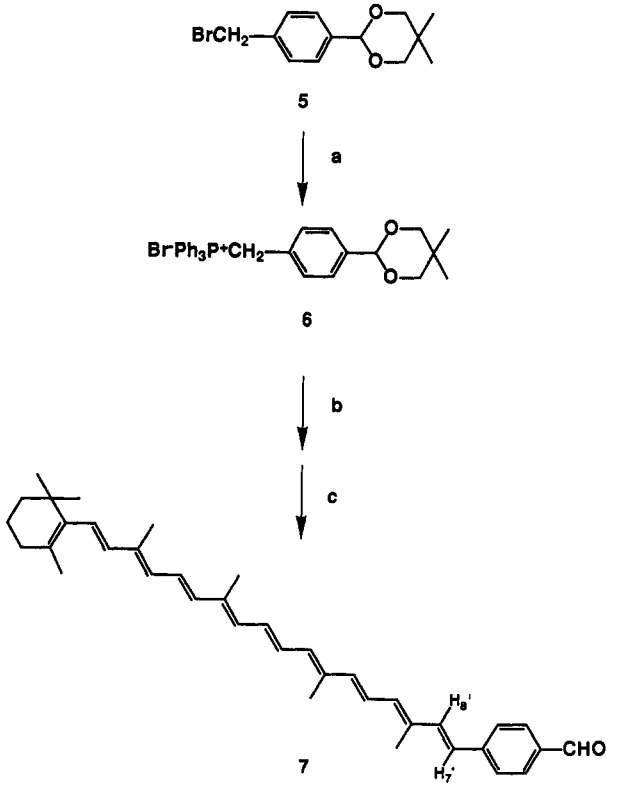

[a] (a) PPh_3, ether, 14 h, room temperature, (b) NaH, MeOH, toluene, 8′-apo-β-carotenal (**4**), reflux, 14 h, in the dark, (c) 1 N HCl, 90 min, room temperature, aqueous $NaHCO_3$.

Experimental Section. They are, however, included in the supplementary material accompanying this paper. In a similar manner, carotenoid–porphyrin–pyromellitimide triads (C–P–Im) were prepared by the reaction of a carotenoid-substituted aromatic aldehyde and *N*-hexyl-*N*′-(4-formylphenyl)methyl)pyromellitimide (**3**) with **1** (Scheme I).

Benzanilide-bridged molecules C–P(Am) and C–P–Im(Am) were prepared by condensation of amino-substituted porphyrins **14** and **16** with carotenoid-substituted benzoic acid **9**[17b] in the presence of 6-chloro-2,4-dimethoxy-1,3,5-triazine (CDMT).[30]

It should be noted that most of the models reported here are rather unstable and were stored in the dark under a nitrogen atmosphere at liquid nitrogen temperature. Even under such strict conditions, we observed spectral changes in the visible absorption bands of C–P, particularly at the absorption of C after several weeks. Thus we repeatedly prepared fresh sample just prior to all measurements.

Optical Properties. UV–visible spectra of some of the compounds synthesized are shown in Figure 1. Complete UV-visible data for the other porphyrins are given in the Experimental Section (Table II). Practically similar absorption spectral changes were observed for C–H_2P and C–ZnP dyads. Figure 1 shows the absorbances of C–ZnP(14B), C–ZnP(P1), and a equimolar mixture of zinc 5,15-(4-methylphenyl)-2,8,12,18-tetrahexyl-3,7,-13,17-tetramethylporphinate (**12**) and 7′-apo-7′-(4-methylphenyl)-β-carotene (**8**) being normalized at 585 nm. Absorbances of both porphyrin (Soret band and Q-bands) and carotenoid (^{1}Bu) chromophores were observed in the absorption spectra of the dyads. Although the peak maxima of the absorption spectrum of C–ZnP(P1) are almost the same as those of the reference mixture of **8** and **12**, the spectrum of C–ZnP(14B) exhibits slight red shifts, especially at the absorption bands of the carotenoid, owing to the conjugation with a spacer of the phenyl group. Observed red shifts in C–ZnP(14B) were ca. 2 nm at the Soret band and 5 mm at the longest wavelength peaks of the vibrational structure of the carotenoid absorption band. Broadening of the absorption bands of both C and ZnP was also recognized. These observations suggest the existence of some electronic interactions between C and ZnP in C–ZnP(14B). On the other hand, the electronic interaction between C and ZnP is negligibly weak in C–ZnP(P1). Spectral red shifts and broadening were also

(30) Kaminskin, Z. J. *Synthesis* **1987**, 917.

Chart III. Structures of Carotenoids **8–10** and Porphyrins **11–16**

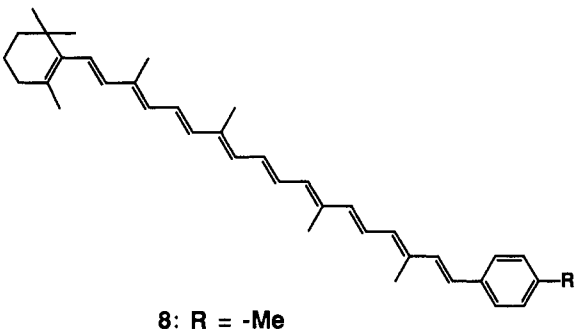

8: R = -Me

9: R = $-CO_2H$

10: R = -NHCOMe

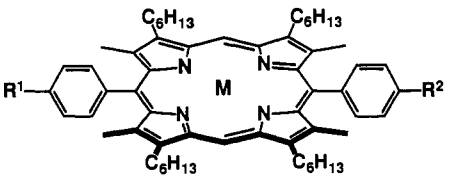

11: $R^1 = R^2$ = -Me, M = H_2

12: $R^1 = R^2$ = -Me, M = Zn

13: R^1 = MeCONH-, R^2 = -Me, M = H_2

14: $R^1 = H_2N$-, R^2 = -Me, M = H_2

15: R^1 = MeCONH-, R^2 = -Im, M = H_2

16: $R^1 = H_2N$-, R^2 = -Im, M = H_2

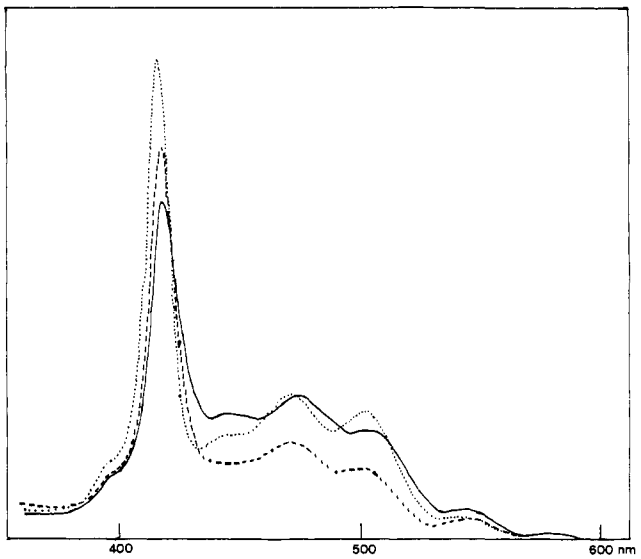

Figure 1. Absorption spectra of C–ZnP(14B) (—), C–ZnP(P1) (- - -), and an equimolar mixture of **8** and **12** (···) in THF.

Table I. Fluorescence Lifetimes and Rate Constants of Singlet–Singlet Energy Transfer in Dyads C–H_2P and C–ZnP

		H_2P			ZnP	
spacer	A^a	k_1 (s^{-1})^b	τ(H_2P) (ns)^c	k_2 (s^{-1})^d	τ(ZnP) (ps)^e	k_5 (s^{-1})^f
14B	35	5×10^{10}	0.84(0.87)	2.8×10^9	83(0.84)	1.1×10^{10}
13B	22	3×10^{10}	2.4(0.84)	4.0×10^8	320(0.78)	2.5×10^9
26N	26	4×10^{10}	1.7(0.67)	7.5×10^8	210(0.69)	4.1×10^9
27N	31	5×10^{10}	3.5(0.82)	2.5×10^8	410(0.85)	1.8×10^9
4P04	18	2×10^{10}	3.5(0.79)	2.0×10^8	480(0.73)	1.4×10^9
3P04	14	2×10^{10}	6.1(0.63)	7.5×10^7	830(0.70)	5.4×10^8
4P03	15	2×10^{10}	5.8(0.42)	1.0×10^8	660(0.80)	8.5×10^8
P1	10	1×10^{10}	6.8(0.78)	5.0×10^7	910(0.91)	4.3×10^8
1S5	9	1×10^{10}	6.7(0.78)	7.5×10^7	660(0.70)	8.5×10^8
1S6	30	3×10^{10}	6.2(0.63)	1.0×10^8	600(0.83)	1.0×10^9
Am	12	1×10^{10}	8.2(0.98)	2.5×10^7	660(0.80)	8.5×10^8

^{a} Efficiency of the intramolecular EN from ^{1}(C)* to H_2P determined by comparison of the absorption spectra and corrected excitation fluorescence spectra. ^{b} Rates of the intramolecular EN from ^{1}(C)* to H_2P calculated by eq 1. ^{c} The fluorescence lifetime of the H_2P in C-H_2P, λ_{em} = 700 nm. Numbers in parentheses are the relative amplitudes in the biexpoential function. ^{d} Rates of the intramolecular EN from ^{1}(H_2P)* to C calculated by eq 5. ^{e} The fluorescence lifetime of the ZnP in C–ZnP, λ_{em} = 585 nm. ^{f} Rates of the intramolecular EN from ^{1}(ZnP)* to C calculated by eq 6.

observed for other C–P dyads, with the exception of C–P(1S5) and C–P(1S6). A common structural feature of dyads which lack electronic interactions between C and P is the presence of an aliphatic carbon in the bridge which interrupts the π-conjugation. This, in turn, means that there is some π-conjugation between C and P in C–P dyads bridged by benzene, naphthalene, biphenyl, and benzanilide spacers, in spite of the perpendicular geometry of the porphyrin and meso-ary bridge.[31] It is interesting to note that these electronic interactions are also observed for C–P(Am), probably reflecting the partial π-bond character of an amide linkage.

Figure 2 shows the steady-state fluorescence spectra of the reference free base porphyrin **11**, C–H_2P(14B), and C–H_2P–Im (14B) in THF. Although the spectral profiles remained essentially unchanged upon attachment of C or Im, the fluorescence intensities decrease in the order of **11** > C–H_2P(14B) > C–H_2P–Im(14B). This result suggests the fluorescence quenching of H_2P by C and Im.[32] It should be noted here that, although the absorption bands of C and the Soret band of P in C–P show a little shifts compared with the reference compounds, the fluorescence spectrum of the P does not virtually show such a shift. This fact indicates that the effect of the electronic interaction on the S_1 state is rather small, which allows usual kinetic treatments for the energy transfer between C and P in the linked system as described in the following.

The fluorescence lifetimes of C–H_2P and C–ZnP were measured by a picosecond time-resolved single-photon counting technique. In most cases, the observed decays can be fit to biexponentials with one major fast component and a minor component with a longer lifetime that is quite similar to that of the C-free reference porphyrins. The amplitude of the long-lived component was sensitive to the degree of purification of the sample and therefore most probably represents an impurity, while the short-lived components were detected with rather constant given lifetimes and variable amplitudes. We, thus, assigned the fast decay component to the fluorescence of intact C–P dyads and the slow one to some materials in which C has been removed or altered.

(31) Almost perpendicular geometries of the meso-aryl ring relative to the porphyrin plane were observed in X-ray structures of the related models, see: (a) Sessler, J. L.; Johnson, M. R.; Creager, S. E.; Fettinger, J. C.; Ibers, J. A. *J. Am. Chem. Soc.* **1990**, *112*, 9310. (b) Osuka, A.; Nakajima, S.; Nagata, T.; Maruyama, K.; Toriumi, K. *Angew. Chem., Int. Ed. Engl.* **1991**, *30*, 582.

(32) A reviewer suggested that a structure-derived modification in the rate of nonradiative relaxation might cause the reduced fluorescence intensities of ^{1}(H_2P)* in the dyad and triad.

Table II. Absorption Maxima of C–H_2P and C–ZnP

spacer[a]	UV–visible spectra ($\epsilon \times 10^{-3}$) (nm M^{-1})											
	C–H_2P						C–ZnP					
14B	411 (170)	445 (88)	473 (100)	508 (95)	574 (7.2)	630 (1.4)	418 (310)	444 (110)	474 (120)	505 (94)	546 (30)	580 (7.3)
13B	410 (250)	443 (98)	473 (120)	505 (110)	574 (7.2)	630 (1.4)	418 (340)	444 (82)	474 (98)	504 (79)	545 (79)	580 (7.3)
26N	412 (212)	450 (92)	478 (102)	510 (113)	575 (7.2)	630 (1.4)	419 (302)	450 (95)	478 (107)	510 (81)	540 (31)	580 (7.3)
27N	412 (210)	450 (92)	477 (110)	509 (106)	575 (7.2)	630 (1.4)	419 (350)	450 (100)	476 (119)	507 (92)	540 (29)	580 (7.3)
4P04	412 (190)	446 (78)	476 (84)	508 (77)	574 (7.2)	630 (1.4)	418 (420)	450 (110)	478 (130)	510 (100)	545 (32)	580 (7.3)
4P03	410 (244)	450 (90)	476 (107)	506 (99)	575 (7.2)	630 (1.4)	418 (440)	450 (93)	470 (110)	500 (80)	545 (23)	580 (7.3)
3P04	410 (250)	440 (96)	470 (117)	503 (108)	575 (7.2)	630 (1.4)	418 (435)	440 (100)	469 (126)	500 (97)	545 (24)	580 (7.3)
P1	409 (250)	440 (90)	469 (110)	503 (98)	575 (7.2)	630 (1.4)	418 (440)	sh[b]	470 (110)	500 (80)	545 (23)	580 (7.3)
1S5	410 (250)	442 (72)	470 (77)	504 (76)	575 (7.2)	630 (1.4)	417 (445)	440[sh] (78)	470 (83)	500 (66)	545 (23)	580 (7.3)
1S6	410 (250)	445 (92)	472 (117)	504 (110)	575 (7.2)	630 (1.4)	418 (463)	445 (90)	470 (115)	500 (94)	545 (23)	580 (7.3)
AMD	411 (208)	452[sh] (92)	478 (122)	508 (116)	575 (7.2)	630 (1.4)	417 (390)	450 (88)	476 (115)	507 (95)	545 (28)	580 (7.3)

spacer[a]	UV–visible spectra ($\epsilon \times 10^{-3}$) (nm M^{-1})					
	C-H_2P-Im					
14B	410 (180)	450 (100)	475 (140)	508 (130)	575 (7.2)	630 (1.4)
P1	410 (252)	440 (81)	468 (94)	502 (85)	575 (7.2)	630 (1.4)
AMD	410 (214)	450[sh] (80)	475 (101)	506 (96)	575 (7.2)	630 (1.4)

[a] Spacer abbreviation depicted in Chart I. [b] sh means shoulder.

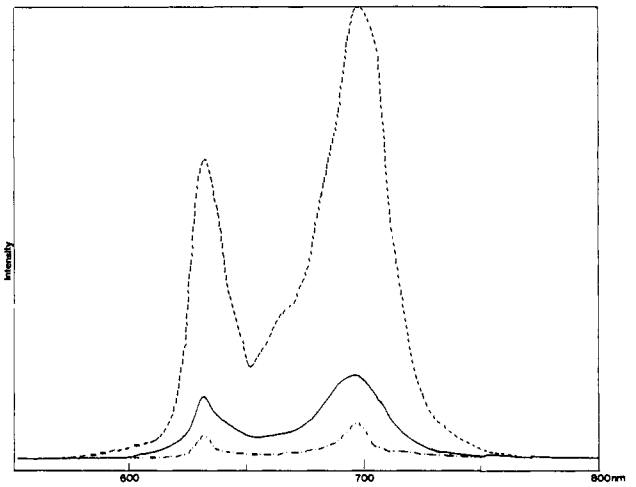

Figure 2. Steady-state fluorescence spectra of **11** (- - -), C-H_2P(14B) (—), and C-H_2P-Im(14B) (---) for excitation at 585 nm in THF.

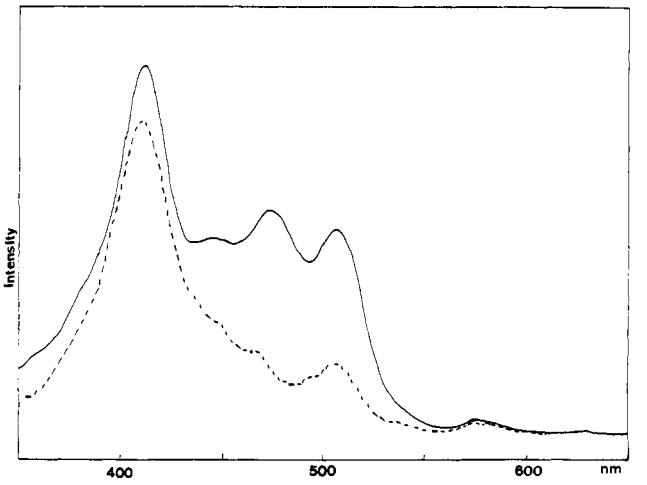

Figure 3. Absorption spectrum (—) and corrected fluorescence excitation spectrum (- - -) of C-H_2P(14B) in THF. The corrected fluorescence excitation spectrum was taken by monitoring the porphyrin fluorescence at 698 nm.

This sort of matter is inevitable for the aromatic molecule bridged carotenoid–porphyrin dyads due to their thermal instability. The lifetimes of the fast components are shown with their relative amplitudes in Table I.

Intramolecular Singlet–Singlet Energy Transfer from C to H_2P. Singlet–singlet excitation energy transfer from the carotenoid to the porphyrin has been recognized as an important process in relation to the natural antenna function of carotenoids. Figure 3 shows the absorption and corrected fluorescence excitation spectra of C–H_2P(14B) in THF solution. The appearance of the carotenoid bands in the excitation spectrum demonstrates that an energy transfer from ^{1}(C)* to H_2P occurs, in competition with very rapid decay of ^{1}(C)*. An energy-transfer efficiency of 35% can be estimated from the ratio of the normalized corrected excitation spectrum to the absorption spectrum.[2,14] Values of energy-transfer efficiency (A) determined similarly for other C–H_2P models are summarized in Table I. Rates (k_1) of the intramolecular singlet–singlet energy transfer from ^{1}(C)* to H_2P were calculated by eq 1, where A is energy transfer efficiency and τ_0(C) is the lifetime of the singlet excited state of the reference carotenoid **8**. We used 10 ps for τ_0(C) for the calculation, since

$$k_1 = \frac{A}{1-A}\frac{1}{\tau_0(\mathrm{C})} \qquad (1)$$

the transient absorption spectroscopy on **8** in THF revealed its singlet lifetime to be about 10 ps (see the following section).

Singlet–Singlet Energy Transfer from ^{1}(H_2P)* to C. Figure 4(a) shows the transient absorption spectra of **8** taken in THF. Excitation of **8** with 532-nm laser light results in an immediate appearance of an absorbance around 572 nm and bleaching at 442, 468, and 500 nm. The bleaching corresponds well to the ground-state absorption of **8**. The absorption at 572 nm, which can be assigned to the $S_n \rightarrow S_1$ transition of **8**,[33-35] decays very rapidly with τ = ca. 10 ps. This lifetime has been determined by deconvolution, taking the excitation pulse width into consideration.

As noted above, the fluorescence of H_2P in C–H_2P was quenched by the attached carotenoid. In order to examine the mechanism of this fluorescence quenching, we observed picosecond time-resolved transient absorption spectra of C–H_2P. Typically, Figure 5 shows the transient absorption spectra of C–H_2P(14B) taken in THF for excitation at 585 nm, where the H_2P only was excited. In the region below 540 nm, we could not obtain meaningful spectra because of very strong bleachings of C. The transient absorption spectrum at 20-ps delay time apparently contains a considerable absorbance around 572 nm in addition to the

(33) Wasielewski, M. R.; Kispert, L. D. *Chem. Phys. Lett.* **1986**, *128*, 238.
(34) A slightly shorter lifetime (8.1 ± 0.5 ps) was reported in 3-methylpentane: Wasielewski, M. R.; Johnson, D. G.; Bradford, E. G.; Kispert, L. D. *J. Chem. Phys.* **1989**, *91*, 6691.
(35) Hashimoto, H.; Koyama, Y.; Hirata, Y.; Mataga, N. *J. Phys. Chem.* **1991**, *95*, 3072.

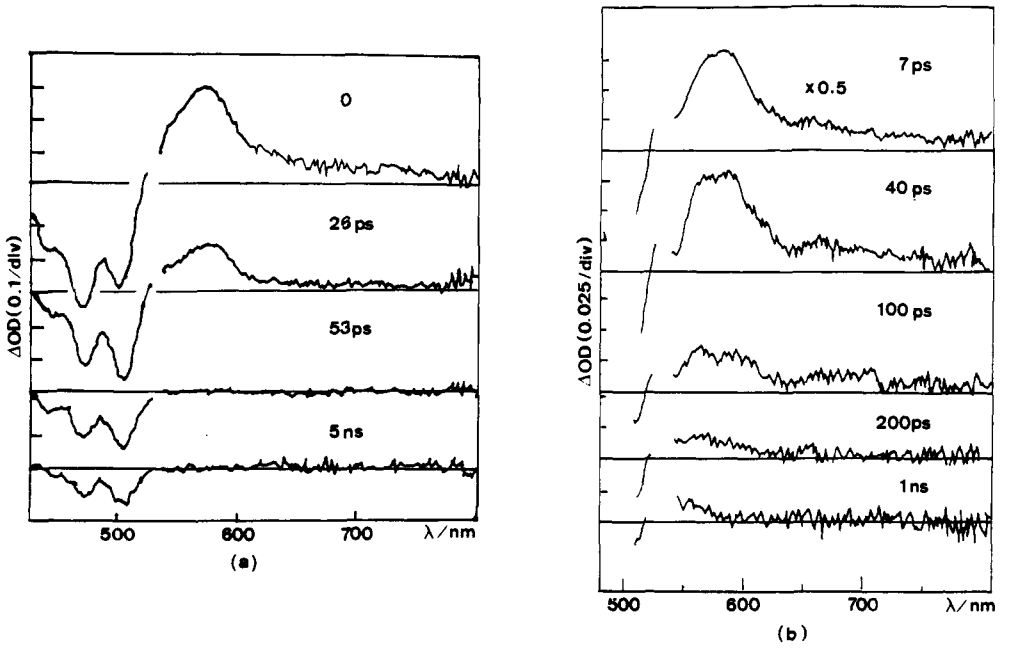

Figure 4. (a) Transient absorption spectra of **8** for excitation at 532 nm in THF. (b) Transient absorption spectra of C-ZnP(14B) for excitation at 532 nm in THF.

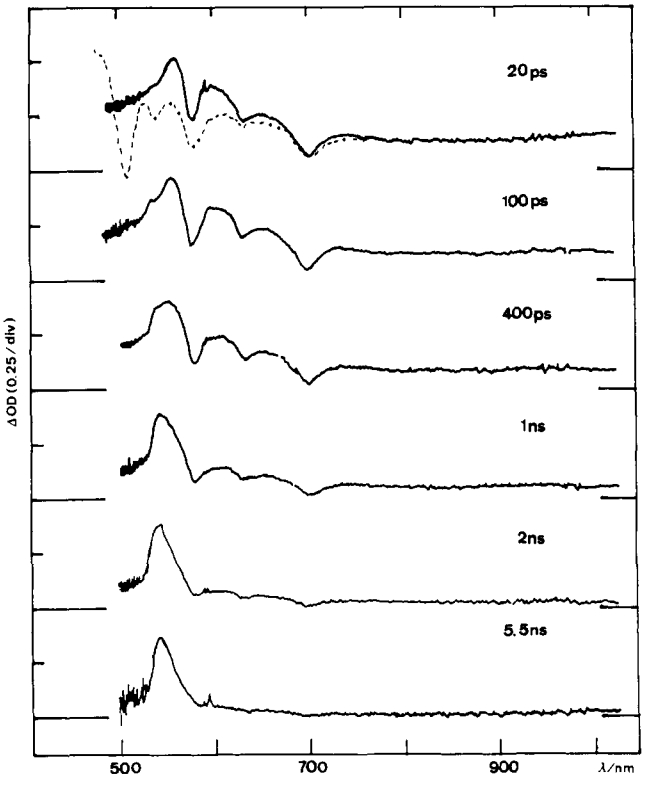

Figure 5. Transient absorption spectra of C-H_2P(14B) for excitation at 585 nm in THF.

absorbance due to $^1(H_2P)^*$, which is shown by a broken line in Figure 5. The absorbance around 572 nm, which decayed with τ = 930 ps, was assigned to $^1(C)^*$. Since the intrinsic lifetime of $^1(C)^*$ is very short (ca. 10 ps), the observed decay rate of the absorbance around 572 nm has been interpreted to reflect the energy transfer from $^1(H_2P)^*$ to C, by which $^1(C)^*$ is populated with a much slower rate than its fast decay. In accordance with this interpretation, the fluorescence lifetime of the H_2P in C–H_2P is 850 ps, being similar to the decay time of the absorbance due to $^1(C)^*$ at 572 nm. The energy transfer from $^1(H_2P)^*$ to C with a slower rate ($<2 \times 10^8$ s^{-1}) was observed in the transient absorption spectra of C–H_2P(P1) under the same conditions. In this case also, the fluorescence lifetime of the H_2P (6.8 ns) in C–H_2P(P1) is roughly similar to that of the observed decay of the absorbance at 572 nm. On the basis of these findings, we conclude that is C–H_2P studied here the intramolecular singlet–singlet EN from $^1(H_2P)^*$ to C is the main quenching process. The singlet excited state $^1(C)^*$ thus formed from $^1(H_2P)^*$ again undergoes intramolecular EN to produce $^1(H_2P)^*$ in competition with its rapid internal conversion to the ground state. Therefore the singlet–singlet EN between C and H_2P is reversible.

We have attempted to determine the rates of the intramolecular singlet–singlet EN from $^1(H_2P)^*$ to C by considering the reaction scheme depicted in Scheme III(a). Assuming energy transfer in both directions between C and H_2P, the time dependence of $[C\text{-}^1(H_2P)^*]$ is written as follows:

$$[C\text{-}^1(H_2P)^*] = C_1 \exp(-\alpha t) + C_2 \exp(-\beta t) \qquad (2)$$

$$\alpha = {}^1/_2[k_1 + k_2 + k_3 + k_4 + \{(-k_1 + k_2 - k_3 + k_4)^2 + 4k_1k_2\}^{1/2}] \qquad (3)$$

$$\beta = {}^1/_2[k_1 + k_2 + k_3 + k_4 - \{(-k_1 + k_2 - k_3 + k_4)^2 + 4k_1\}^{1/2}] \qquad (4)$$

$$C_1 = \frac{k_2 + k_4 - \beta}{\alpha - \beta} \qquad C_2 = \frac{\alpha - k_2 - k_4}{\alpha - \beta} \qquad (5)$$

where k_1, k_2, k_3, and k_4 are defined in Scheme III(a) and C_1, C_2, α, and β are the experimental values that, ideally, can be determined from the fluorescence decay analysis. In principle, an accurate determination of the biexponential fluorescence decay function allows the evaluation of α, β, C_1, and C_2. However, we could characterize only one decaying component besides a slow decay which is presumably due to a carotenoid-altered impurity. Since the sum of k_1 and k_3 is very large, the first exponential term in eq 2, $\exp(-\alpha t)$, is very short-lived (<10 ps) and probably cannot be detected by our instrument. Thus, the decaying component characterized here was related to the other exponential component, $\exp(-\beta t)$, and we have calculated k_2 values from eq 4 with values of k_1 (Table I), $k_3 = 1 \times 10^{11}$ s^{-1}, and $k_4 = 9 \times 10^7$ s^{-1}. The k_2 rates thus determined were summarized in Table I.

Singlet–Singlet Energy Transfer from ^{1}(ZnP)* to C. In contrast to the C–H_2P series, the fluorescence excitation spectra of C–ZnP studied here contain no contribution of absorption of C, indicating

Scheme III. Reaction Scheme for C–H_2P (a) and C–ZnP (b)

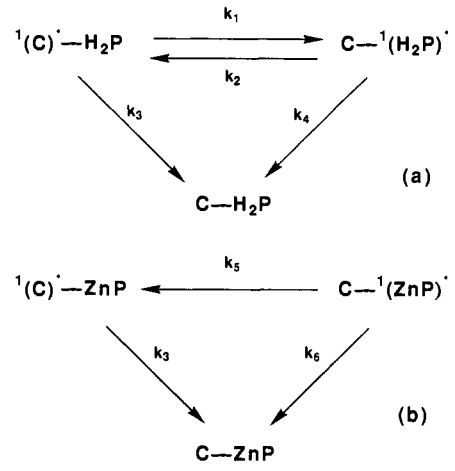

the absence of the intramolecular EN from ^{1}(C)* to ZnP. As noted above, the fluorescence of ZnP was also quenched by the attached carotenoid. Figure 4(b) shows the transient absorption spectra of C–ZnP(14B) taken in THF for excitation at 532 nm, where both C and ZnP were excited. The absorption at 572 nm for C–ZnP(14B) shows a double-exponential decay with $\tau \sim 10$ and 70 ps. We interpret these two time constants as the decay of ^{1}(C)* formed by the exciting pulse and the decay of ^{1}(C)* formed by intramolecular singlet–singlet energy transfer from ^{1}(ZnP)*, respectively. In order to confirm this interpretation, we examined similar transient absorption spectra of C–ZnP(14B) by exciting at 585 nm (Figure 6), where only the ZnP moiety was excited. The spectral feature at 20-ps delay time indicated the formation of ^{1}(C)* (absorbance around 572 nm) as well as ^{1}(ZnP)* (absorbance around at 590 nm and induced emission at 540 nm) immediately after excitation. Thus it is now again apparent that the ^{1}(C)*–ZnP state is formed from the C–^{1}(ZnP)* state.[36] The absorbance at 572 nm decayed with $\tau = 70$ ps, being similar to the fluorescence lifetime of ZnP (83 ps) in C-ZnP(14B). Thus the energy transfer from ^{1}(ZnP)* to C has been also observed as the main quenching process for the ^{1}(ZnP)* in C–ZuP(P1) by transient absorption experiments.

Assuming the reaction scheme shown in Scheme III(b), the rate of the intramolecular singlet–singlet energy transfer (k_5) can be calculated by eq 6, where τ(ZnP) is the fluorescence lifetime

$$k_5 = 1/\tau(\mathrm{ZnP}) - 1/\tau_0(\mathrm{ZnP}) \qquad (6)$$

of ZnP in C–ZnP and τ_0(ZnP) = k_6^{-1} is the fluorescence lifetime of the reference ZnP (1.32 ns in THF). The rates (k_5) of the intramolecular EN from ^{1}(ZnP)* to C thus calculated are summarized in Table I.

Photoexcited-State Dynamics of C–H_2P–Im. Figure 7 shows the transient absorption spectra of C–H_2P–Im(14B) taken in THF for excitation at 532 nm. It should be worth noting that both absorption bands due to (Im)$^-$ at 715 nm and (C)$^+$ over 900 nm were distinctly observed in the 40-ps $\sim$ 5-ns time region. The bleachings at 446, 470, and 505 nm were also observed in the same time region. These observations provide clear evidence for the rapid formation of a charge-separated state (C)$^+$–H_2P–(Im)$^-$ in several tens of picoseconds. A lifetime of this charge-separated state, (C)$^+$–H_2P–(Im)$^-$, was determined by nanosecond transient absorption spectroscopy to be 11 ns. In a C-free H_2P–Im reference compound, electron transfer from ^{1}(H_2P)* to Im proceeds with a rate constant of 9.2×10^7 s^{-1} (the fluorescence lifetime of the reference H_2P–Im is 5.2 ns in THF).[28c] Thus the initial charge separation between ^{1}(H_2P)* and Im and subsequent hole transfer from (H_2P)$^+$ to C cannot explain the rapid formation of

(36) Intramolecular EN from the singlet excited state of zinc porphyrin to the attached polyene was also reported in ref 28c.

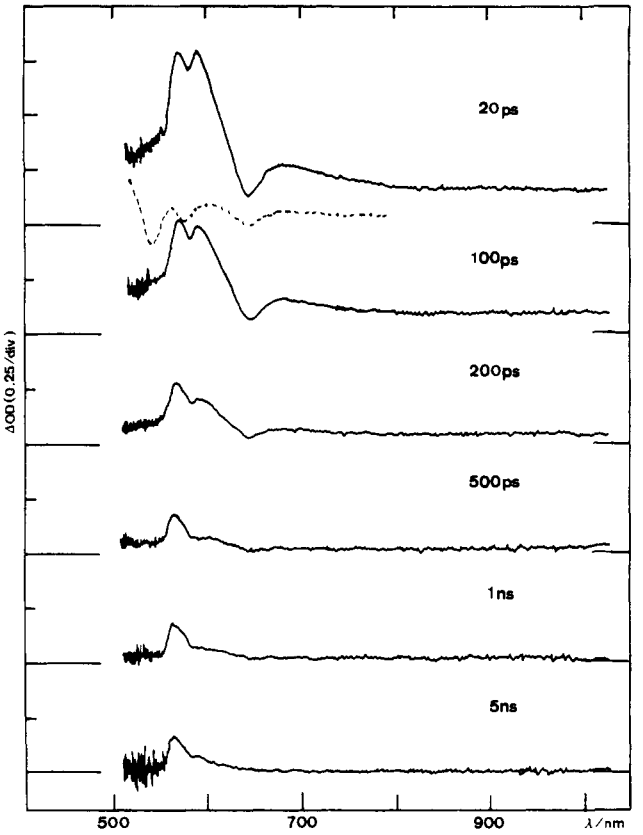

Figure 6. Transient absorption spectra of C–ZnP(14B) for excitation at 585 nm in THF.

(C)$^+$–H_2P–(Im)$^-$ in several tens of picoseconds. In fact, the fluorescence lifetime of the ^{1}(H_2P)* in C–H_2P–Im(14B) is 770 ps, being much longer than the rise time of the (C)$^+$–H_2P–(Im)$^-$ state. Thus the rapid accumulation of the (C)$^+$–H_2P–(Im)$^-$ state is likely to indicate the long-distance electron transfer from ^{1}(C)* to Im. Figure 8 shows the transient absorption spectra of C–H_2P–Im(14B) for excitation at 585 nm, where only the H_2P was excited. In these spectra, the formation of (C)$^+$–H_2P–(Im)$^-$ was also observed but the time constant for its formation (ca. 700 ps) was much slower, compared to the case for excitation at 532 nm. This time constant for the formation of (C)$^+$–H_2P–(Im)$^-$ is quite similar for the fluorescence lifetime of the H_2P in C–H_2P–Im(14B), yet being faster than the electron transfer from ^{1}(H_2P)* to Im, 5.2 ns. Accordingly, the most effective route to (C)$^+$–H_2P–(Im)$^-$ from C–^{1}(H_2P)*–Im involves EN from ^{1}(H_2P)* to C and subsequent, more rapid, long-distance electron transfer from ^{1}(C)* to Im. In C–H_2P–Im(14B), the center-to-center distance of C and Im is as long as 28 Å and the edge-to-edge distance is 14 Å, and thus such rapid electron transfer is somewhat surprising. In related triads such as C–H_2P–Im(P1) and C–H_2P–Im(Am), the ^{1}(H_2P)* decayed with lifetime of ca. 3 $\sim$ 5 ns upon excitation at either 532 or 585 nm,[37] but nevertheless a rapid rise of the absorbances due to (C)$^+$–H_2P–(Im)$^-$ with time constants of several tens of picoseconds was observed only upon excitation at 532 nm. Upon excitation at 585 nm, the formation of the (C)$^+$–H_2P–(Im)$^-$ state took more time: ca. 3 and 4 ns in C–H_2P–Im(P1) and C–H_2P–Im(Am), respectively. Thus we concluded that a long-distance electron transfer from ^{1}(C)* to Im was also responsible for such a rapid formation of (C)$^+$–H_2P–(Im)$^-$ in these triads for excitation at 532 nm. (C)$^+$–H_2P–(Im)$^-$(P1) and (C)$^+$–H_2P–(Im)$^-$(Am) thus formed undergo charge recombination with rates of 2.8×10^6 and 6.7×10^6 s^{-1}, respectively.

(37) The fluorescence lifetimes of the H_2P in C–H_2P–Im(P1) and C–H_2P–Im(Am) were 3.6 and 4.4 ns, respectively, in agreement with the results of the transient absorption experiments.

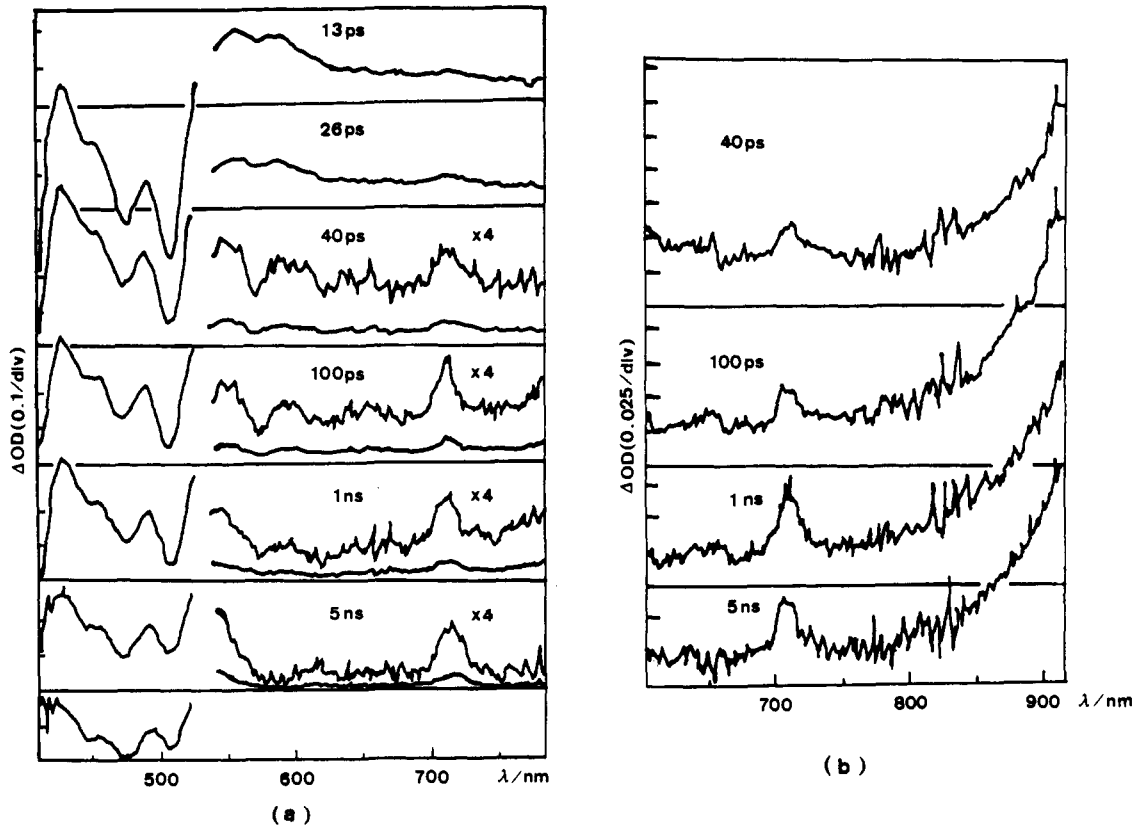

Figure 7. Transient absorption spectra of C-H_2P-Im(14B) for excitation at 532 nm in THF: (a) in 430-780 nm and (b) in 630-930 nm.

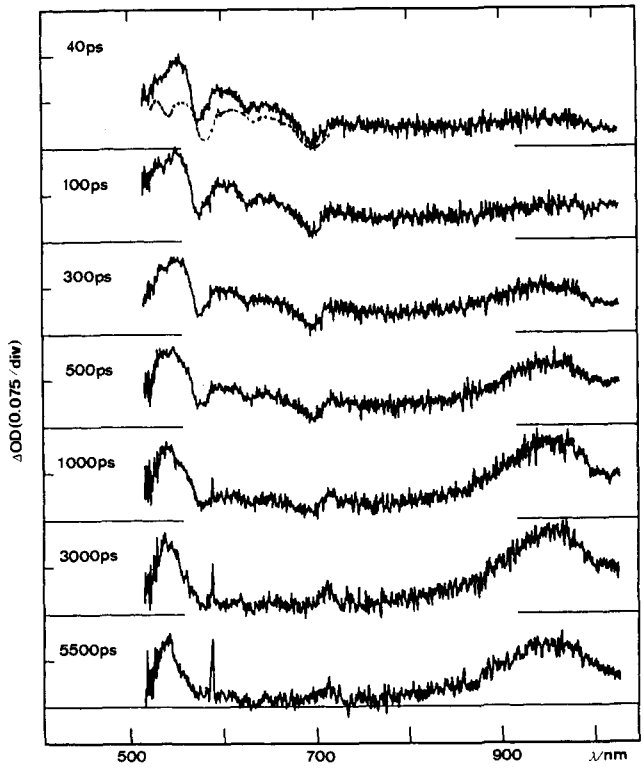

Figure 8. Transient absorption spectra of C-H_2P-Im(14B) for excitation at 585 nm in THF.

Discussion

Intramolecular Singlet–Singlet Energy Transfer. The results of these studies show that intramolecular singlet–singlet EN proceeds in both directions between C and H_2P, while only one-way singlet–singlet EN from ^{1}(ZnP)* to C takes place in C–ZnP dyads. Although quenching of porphyrin fluorescence by the attached carotenoid has been recognized for long time, its mechanism was not clear. Intramolecular electron transfer to the singlet excited state of the porphyrin from the attached carotenoid was suggested as a possibility for the quenching mechanism.[23e] This seems to be based on the original attribution of the quenching of the chlorophyll first excited singlet state by β-carotene.[38] In a special C–P model where an expected charge-separated state lies at an energy level which is sufficiently lower than that of the singlet excited state of the porphyrin, intramolecular electron transfer from the attached carotenoid to the porphyrin has indeed been detected by transient absorption spectroscopy in *n*-butyronitrile.[39] Recently, on the basis of evidence indicating no significant changes in fluorescence radiative rates constant nor in intersystem crossing rates, electron transfer, singlet–singlet energy transfer from porphyrin to carotenoid, and enhanced nonradiative deactivation were proposed as three alternative explanations to the quenching.[18] The results presented here showed more clearly that the singlet–singlet energy transfer is principally responsible for the fluorescence quenching of the porphyrin, at least in the present aromatic group-bridged carotenoid–porphyrin dyads, which will be followed by the very rapid internal conversion to the ground state within C.

We have estimated rates of three different EN processes, k_1, k_2, and k_5, for all the dyads (Table I and Figure 9). Two key features are readily apparent: (1) although the rates of the three EN processes are different from one another, their spacer dependencies exhibit similar trends, particularly the similarity of k_2 and k_5 is remarkable, and (2) the rates of these EN processes remain in the order of $k_1 > k_5 > k_2$ for all dyads bridged by the same spacer. We will discuss the mechanisms of these EN processes by taking these features into consideration. In esti-

(38) Beddard, G. S.; Davidson, R. S.; Trethewey, K. R. *Nature* **1977**, *267*, 373.

(39) (a) Gust, D.; Moore, A. L.; Moore, T. A.; Lin, S.; Hermant, R. M.; Liddell, P. A.; Alden, R. G. *Photosynth. Res.* **1992**, *34*, 165. After the first submission of this manuscript, a related paper reporting a distinct detection of a charge-separated state by transient absorption spectroscopy appeared, see: (b) Herman, R. M.; Liddell, P. A.; Lin, S.; Alden, R. G.; King, H. K.; Moore, A. L.; Moore, T. A.; Gust, D. *J. Am. Chem. Soc.* **1993**, *115*, 2080.

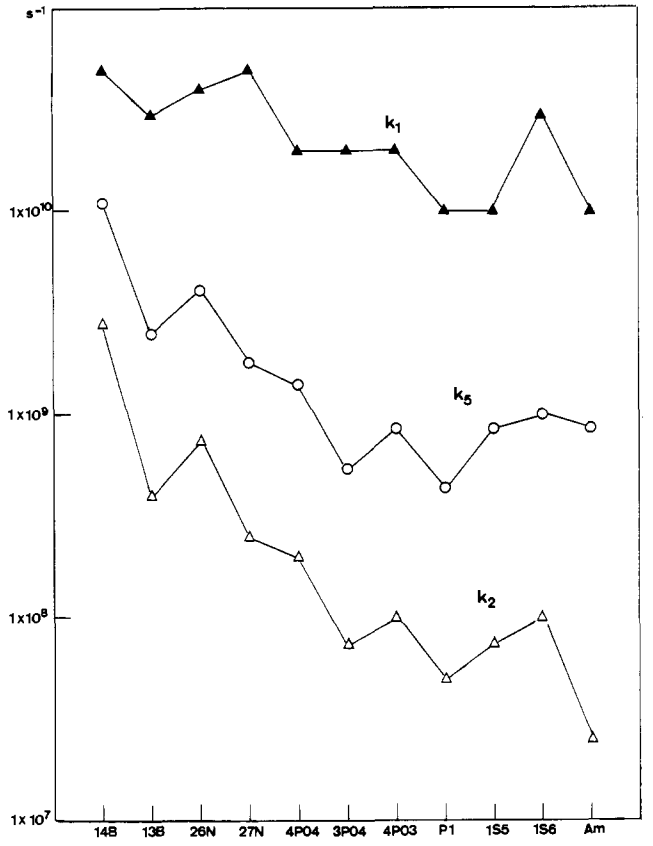

Figure 9. Spacer dependencies of k_1 (▲), k_2 (△), and k_5 (○).

mation of k_1 and k_2, we used 10 ps for a lifetime of the first singlet excited state of C on the basis of the results for **8**. Recent transient absorption experiments have the S_1 lifetime to be 8.4 ± 0.6 ps in toluene[33,34] and 12.4 ± 0.5 ps in *n*-hexane[35] for *all-trans*-β-carotene, and 15 ps for spheroidenone in CS_2.[40] On the other hand, the S_1 lifetime of the closely related polyene **10** was reported to be 16 ps.[20] Therefore, the lifetime of $^1(C)^*$ used here seems consistent with other reports.[41]

It is very important to estimate the excitation energies of the singlet excited states of C. Carotenoids are expected to have two energetically low-lying singlet states, the 1^1B_u and 2^1A_g states.[42] The former state is dipole allowed from the ground state, while the latter state of a symmetric carotenoid is formally dipole forbidden. The ground-state absorption bands at 442, 468, and 500 nm of **8** are probably due to a fully allowed dipole transition to its 1^1B_u state (S_2), while the lowest excited singlet state of **8** must be an 2^1A_2 state, which is much lower in energy than its 1^1B_u state. The excitation energy of the S_2 state of C was estimated, on the basis of the spectroscopic data of **8**, to be ca. 2.45 eV, while no spectroscopic data are available for the S_1 state. The S_1 state of **8**, in which the symmetry is formally broken, would be less forbidden, but the fluorescence of **8** was virtually undetectable, indicating the fluorescence quantum yield being less than $<10^{-5}$. Since the S_2 state of C, judging from recent ultrafast spectroscopic experiments on related molecules, seems to be very short-lived (on order to 100–200 fs)[40,43,44] compared to the EN to the attached porphyrins observed here, it is reasonable to assume that essentially all of the EN reactions reported here involve the S_1 state of C.

With regard to the energy level of the S_1 state of C, we consider its location between the S_1 states of H_2P (1.97 eV) and ZnP (2.13 eV) from the following reasons: (1) reversible singlet–singlet EN reactions between C and H_2P suggest that the S_1 state of C is nearly isoenergetic to that of $^1(H_2P)^*$,[55] and much larger values of k_1 in comparison with k_2 indicate that the $^1(C)^*$ state lies slightly higher in energy than $^1(H_2P)^*$ and (2) the one-way EN from $^1(ZnP)^*$ to C indicates the S_1 state of C is dinstinctly lower in energy than that of $^1(ZnP)^*$.

Two major mechanisms for singlet–singlet energy transfer have been identified. The Förster mechanism operates via Coulombic interaction between transition dipole moments and therefore requires no direct contact between the energy donor and acceptor,[46] while the Dexter mechanism depends on electron exchange and thus requires spatial overlap.[47,48] In both mechanisms the energy transfer depends on the spectral overlap between the absorption band of the acceptor and the fluorescence emission band of the donor. The rate of the Förster mechanism depends additionally on the donor fluorescence quantum yield. It is very important to distinguish these two mechanisms in understanding the mechanism of carotenoid–chlorophyll singlet–singlet energy transfer in photosynthetic organisms.

Inspection of the spacer dependencies summarized in Table I and Figure 9 sheds light on the mechanisms of these EN processes. We shall restrict our discussion to the spacer dependencies of k_5, since these values are the most reliable of the three series. But the similarity of the spacer dependencies of k_1 and k_2 to that of k_3 indicates that an analogous interaction is also an important factor in the three EN processes. Comparisons of k_5 rates for C–ZnP(14B) and C–ZnP(13B) or for C–ZnP(26N) and C–ZnP(27N), and for C–ZnP(4P04), C–ZnP(4P03), and C–ZnP(3P04), are quite interesting (the order is evidence from Table I and Figure 9 as follows, C–ZnP(14B) > C–ZnP(13B), C–ZnP(26N) > C–ZnP(27N), and C–ZnP(4P04) > C–ZnP(4P03) > C–ZnP(3P04). In these models, the electronic π-system of a carotenoid is conjugated with the meso-aryl bridge, and thus the electronic π-system of the carotenoid is *directly attached to* the porphyrin with a somewhat perpendicular arrangement. This causes changes such as red shifts and broadening of the absorption bands, reflecting electronic interactions between C and P to some extent. Therefore, if we postulate that the EN takes place mainly via through-bond electronic exchange coupling, the trend of C–ZnP(14B) > C–ZnP(13B) can be readily explained, since the electronic coupling of the chromophores at the para position to the C should be stronger than that in the meta position in view of much greater orbital density at the para compared to the meta. An analogous explanation would be also valid for the naphthalene- or biphenyl-bridged series. This explanation is also in accordance with the dipole-forbidden nature of the S_1 (2^1A_g) state of C, since the electronic exchange interaction may be principally effective for EN involving such dipole-forbidden states.[47,48] It should be noted here that the excitation energy transfer probability in general depends on the Franck–Condon (FC) factor and the matrix element of the electronic interaction between the energy donor and acceptor. For the energy transfer by the exchange interaction, the matrix element may be concerned with both the LUMO–LUMO overlap and the HOMO–HOMO overlap between the energy donor and acceptors.[47,56,57] For the present compounds,

(40) Gillbro, T.; Cogdell, R. J. *Chem. Phys. Lett.* **1989**, *158*, 312.
(41) A reviewer suggested that, in cases where the spectral perturbation which occurs upon linkage of the carotenoid to the porphyrin is large, a significant change in lifetime in the absence of energy transfer might occur.
(42) Hudson, B. S.; Kohler, B. E.; Schulten, K. Linear Polyene Electronic Structure and Potential Surfaces. In *Excited States*; Lim, E. C., Eds.; Academic Press: New York, 1982; Vol. 6, pp 1.
(43) Shreve, A. P.; Trautman, J. K.; Owens, T. G.; Albrecht, A. C. *Chem. Phys. Lett.* **1991**, *178*, 89.
(44) Shreve, A. P.; Trautman, J. K.; Owens, T. G.; Albrecht, A. C. *Chem. Phys. Lett.* **1991**, *154*, 171.
(45) Thrash, R. J.; Fang, H. L. B.; Leroi, G. E. *J. Chem. Phys.* **1977**, *67*, 5930.
(46) Förster, T. *Discuss. Faraday Soc.* **1959**, *27*, 7.
(47) Dexter, D. L. *J. Chem. Phys.* **1953**, *21*, 836.
(48) Razi-Naqvi, K. *Photochem. Photobiol.* **1980**, *31*, 523.
(49) (a) Friesner, R. A.; Won, Y. *Biochim. Biophys. Acta* **1989**, *977*, 99. (b) Plato, M.; Möbius, K.; Michel-Beyerele, M. E.; Bixon, M.; Jortner, J. J. *J. Am. Chem. Soc.* **1988**, *110*, 7279. (c) Marcus, R. A. *Chem. Phys. Lett.* **1987**, *133*, 471. (d) Won, Y.; Friesner, R. A. *Proc. Natl. Acad. Sci. U.S.A.* **1987**, *84*, 5511. Won, Y.; Friesner, R. A. *Biochim. Biophys. Acta* **1988**, *935*, 9. (e) Plato, M.; Möbius, K.; Michel-Beyerele, M. E.; Bixon, M.; Jortner, J. J. *J. Am. Chem. Soc.* **1988**, *110*, 7279.

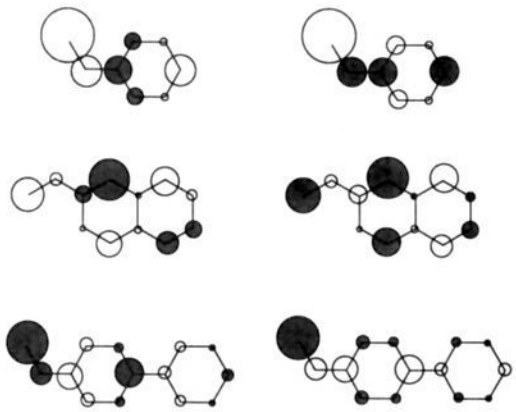

Figure 10. Results of Hückel molecular orbital calculations for the aromatic spacers linking the porphyrin and carotenoid.

the FC factor may be similar throughout the series and the electronic matrix element which depends on the spacer will determine the rate of energy transfer both for P* → C and C* → P processes, in an approximate agreement with the results in Figure 9. In order to illustrate this interpretation, simple Hückel molecular orbital calculations for vinyl-substituted spacers such as styrene, 2-vinylnaphthalene, and 4-vinylbiphenyl have been carried out (Figure 10). The radius of the circle at each atom is proportional to the coefficient of the wave function at that atom, the area is proportional to the orbital density, and the shading reflects the relative sign of the wave function at that point. It is clear that the relative orbital density is in line with the order of k_S. This treatment is quite similar to a recent one reported by Gust and Moore.[18] In their models, the carotenoid is linked to a TPP-type porphyrin not directly but via an amide linkage at the ortho, meta, and para position of a meso aromatic ring. Thus it is likely that more distinct spacer dependencies that are principally mediated by through-bond interaction are observed in our models.

Now it is apparent that even in EN from ^{1}(ZnP)* to C, and presumably in EN's from ^{1}(H_2P)* to C and from ^{1}(C)* to H_2P, the through-bond electronic interaction is dominant in controlling their rates, similar to the related triplet–triplet EN reported by Gust and Moore.[18]

Intramolecular Electron Transfer in C–H_2P–Im. We have also revealed an efficient, one-step, long-distance electron transfer from ^{1}(C)* to Im in C–H_2P–Im triads. It is interesting to note that this long-distance electron transfer has been observed to proceed with similar rates also in P1- or Am-bridged triads, in which the electronic interactions between C and P are less than those in 14B-bridged models. The long-distance electron transfer has been confirmed by experiments with selective excitation at H_2P, since the rise of the final (C)$^+$–H_2P–(Im)$^-$ state from C–^{1}(H_2P)*–Im took a much longer time in comparison with a route starting from ^{1}(C)*–H_2P–Im. Moreover, it is to be noted that the rise of (C)$^+$–H_2P–(Im)$^-$ is yet much faster than an electron transfer from ^{1}(H_2P)* to Im. These facts seem to enforce the existence of the long-distance electron transfer from ^{1}(C)* that is somewhat surprising in view of the long distance (28 Å) between the resulting two charges. One possible explanation for this remarkable process may be that the electronic coupling between the ^{1}(C)*–H_2P–Im state and the (C)$^+$–H_2P–(Im)$^-$ state is enhanced by a superexchange interaction with, for instance, the (C)$^+$–(H_2P)$^-$–Im state as the virtual state. In these systems, the energy of the virtual state, (C)$^+$–(H_2P)$^-$–Im, seems to be very close to that of the initial state, ^{1}(C)*–H_2P–Im, according to the estimation by using the redox potentials, which will facilitate considerably such a superexchange coupling. Similar interpretations in terms of superexchange coupling involving the intervening porphyrin π-orbital have been considered to explain efficient long-distance ET not only in the natural RC systems[45] but also in artificial systems.[29b,31a,50,51]

Formation of long-lived charge-separated states was reported by Gust and Moore in artificial carotenoid–porphyrin–quinone supramolecular arrays.[22,23] It has been reported that such final CT states are formed by a series of short-range, fast, efficient electron-transfer steps triggered by an electron transfer from the singlet excited state of the porphyrin to the attached quinone. In many reported cases where high quantum yields of long-lived CT states have been achieved, it is likely that a secondary electron transfer from the carotenoid to a cation radical of the porphyrin is rapid enough to compete with a wasteful charge recombination reaction within the initially formed carotenoid–(porphyrin)$^+$–(quinone)$^-$ species. The present results pose that, at least in the related C–H_2P–Im triads studied here, another mechanistic possibility exists for the formation of the final CT state, through the direct, long-distance electron transfer from the singlet excited state of the carotenoid to the Im acceptor. We have also shown that the singlet excited state of the carotenoid, in turn, can be formed by the singlet–singlet EN from ^{1}(P)*.

Experimental Section

For synthetic use, acetonitrile was refluxed over and distilled from P_2O_5. Other solvents and reagents were reagent grade. Preparative separations were usually performed by flash column chromatography on silica gel (Merck, Kieselgel 60H, Art. 7736).

UV–visible spectra were recorded with a Shimadzu UV-3000 spectrometer, and steady-state fluorescence and fluorescence excitation spectra were taken on a Shimadzu RF-502A spectrofluorimeter, both at room temperature. Efficiencies of the singlet–singlet energy transfer from ^{1}(C)* to H_2P were determined as follows: (1) the ratios of the normalized corrected excitation spectrum to the absorption spectrum were determined at an interval of 5 nm in a range of 440–540 nm and (2) the obtained values were averaged to get the energy-transfer efficiency (A).[2,14] Even for models where the absorption spectra were somewhat perturbed by the attached carotenoid, the A values were determined within 10% error. ^{1}H-NMR spectra were recorded on a JEOL GX-400 spectrometer (operating at 400 MHz), chemical shifts being reported in the δ scale in ppm relative to Me_4Si. Mass spectra were recorded on JEOL DX-300 and HX-100 spectrometers. For porphyrin compounds, the positive-FAB (fast atom bombardment) ionization method was used, accelerating voltage 1.5 or 10 kV, Xe atom as the primary ion source. The FAB matrix was 3-nitrobenzyl alcohol/chloroform.

Fluorescence lifetimes were measured on 10^{-7} M air-saturated solutions with a picosecond time-correlated single-photon counting system.[52] Picosecond transient absorption spectra were measured on ca. 10^{-4} M nitrogen-bubbled solutions by means of a microcomputer-controlled double-beam picosecond spectrometer with a repetitive, mode-locked Nd^{3+}:YAG laser[53a] or with a picosecond dye laser pumped by the second harmonic of a repetitive, mode-locked Nd^{3+}:YAG laser.[53b] The second harmonic of the Nd^{3+}:YAG laser pulse (24-ps pulse duration) or the 620-nm output of the dye laser (8-ps pulse duration) was used for excitation. A Q-switched Nd^{3+}:YAG laser (Quantel YG580) with second-harmonic output (532 nm, 15-ns pulse duration) of 40 mJ was used for measurements of nanosecond transient absorption spectra. The data-acquisition system has been described elsewhere.[54] Solutions of the triad compounds (ca. 10^{-5} M) were deaerated by bubbling with argon.

(50) Wasielewski, M. R.; Niemczyk, M. P.; Johnson, D. G.; Svec, W. A.; Minsek, D. W. *Tetrahedron* **1989**, *45*, 4785.
(51) Sessler, J. L.; Johnson, M. R.; Lin, T.-Y.; Creager, S. E. *J. Am. Chem. Soc.* **1988**, *110*, 3659. (b) Sessler, J. L.; Johnson, M. R.; Lin, T.-Y. *Tetrahedron* **1989**, *45*, 4767. (c) Rodriguez, J.; Kirmaier, C.; Johnson, M. R.; Friesner, R. A.; Holten, D.; Sessler, J. L. *J. Am. Chem. Soc.* **1991**, *113*, 1652.
(52) Yamazaki, I.; Tamai, N.; Kume, H.; Tsuchiya, H.; Oba, K. *Rev. Sci. Instrum.* **1985**, *56*, 1187.
(53) (a) Miyasaka, H.; Masuhara, H.; Mataga, N. *Laser Chem.* **1983**, *1*, 357. (b) Hirata, Y.; Mataga, N. *J. Phys. Chem.* **1991**, *95*, 1640.
(54) Ohno, T.; Yoshimura, A.; Mataga, N. *J. Phys. Chem.* **1990**, *94*, 4871.
(55) This estimation seems to be consistent with a recent prediction of the S_1 state energy level of a related carotenoid: Cosgrove, S. A.; Guite, M. A.; Burnell, T. B.; Christensen, R. L. *J. Phys. Chem.* **1990**, *94*, 8118.
(56) See, for example: Mataga, N.; Kubota, T. *Molecular Interactions and Electronic Spectra*; Marcel-Dekker: New York, 1970; pp 65–171.
(57) Closs, G. L.; Piotrowiak, P.; Miller, J. R. In *Photochemical* Energy Conversion; Norris, J. R.; Meisel, D., Eds.; Elsevier: Amsterdam, 1989; pp 23.

Synthesis of C–ZnP, C–H_2P, and C–H_2P–Im. Typically, the synthesis of C–ZnP(14B) and C–H_2P(14B) was described. 4-(7′-apo-β-caroten-7′-yl)benzaldehyde (**7**) (40 μmol, 25 mg), **2** (160 μmol, 26 mg), and **1** (200 μmol, 68 mg) were dissolved in a mixture of dry C_6H_6 (4.5 mL) and CH_3CN (10.5 mL). To this solution was added trichloroacetic acid (42 μmol, 6.8 mg) in CH_3CN (68 μL), and the resulting mixture was stirred for 5 h at room temperature under an argon atmosphere in the dark. A solution of *p*-chloranil (0.3 mmol, 80 mg) in dry THF (30 mL) was added, and the mixture was stirred for an addition 2 h. Purification with an alumina short column (5 cm, CH_2Cl_2) was done in order to remove some polymeric materials. Fractions containing porphyrin and/or carotenoid were combined, and the solvent was removed on the rotary evaporator. The residue was dissolved in CH_2Cl_2 (20 mL), and a saturated solution of $Zn(OAc)_2$ in methanol (0.5 mL) was added. The mixture was stirred for several minutes at room temperature under a nitrogen atmosphere in the dark. The solvent was removed by the rotary evaporator, and the residue was separated by flash column chromatography (MeOH-free CH_2Cl_2). Recrystallization from CH_2Cl_2–MeOH gave C–ZnP(14B) (45 mg, 32 μmol, 81% yield based on the amount of **1** used). ^{1}H-NMR ($CDCl_3$): 10.14 (s, 2 H, meso), 8.42 (d, 2 H, J = 8.1 Hz, Ar), 8.10 (d, 2 H, J = 8.1 Hz, Ar), 8.00 (d, 2 H, J = 8.1 Hz, Ar), 7.84 (d, 2 H, J = 8.1 Hz, Ar), 7.24 (d, 1 H, J = 15.8 Hz, Car-H_7′), 6.97 (d, 1 H, J = 15.8 Hz, Car-H_8′), 6.79 (dd, 1 H, J = 15.4 and 14.8 Hz, Car-H_{11}′), 6.7 (m, 3 H, Car), 6.52 (d, 2 H, J = 12.0 Hz, Car), 6.37 (d, 1 H, Car), 6.3 (m, 1 H, Car), 6.27 (m, 1 H, Car), 6.1–6.2 (m, 3 H, Car), 4.14 (s, 3 H, ester-Me), 3.9 (m, 8 H, 4Hex-1-CH_2), 2.52 (s, 6 H, 2Me), 2.41 (s, 6 H, 2Me), 2.23 (s, 3 H, Car-Me), 2.16 (m, 8 H, 4Hex-2-CH_2), 2.05 (s, 3 H, Car-Me), 2.0 (m, 2 H, Car-CH_2), 2.0 (s, 3 H, Car-Me), 1.99 (s, 3 H, Car-Me), 1.73 (m, 8 H, 4Hex-3-CH_2), 1.74 (s, 3 H, Car-Me), 1.6 (m, 2 H, Car-CH_2), 1.5 (m, 10 H, 4Hex-4-CH_2 and Car-CH_2), 1.4 (m, 8 H, 4Hex-5-CH_2), 1.04 (s, 6 H, 2Car-Me), 0.91 (t, 12 H, J = 7.3 Hz, 4Hex-6-Me). HRMS (FAB): found, m/z 1386.858; calcd for $C_{93}H_{118}N_4O_2Zn$, m/z 1386.855 (M^+).

C–H_2P(14B). C–ZnP(14B) was dissolved in CH_2Cl_2, and the resulting solution was shaken in a separatory funnel with 1 N HCl a few times. The organic layer was separated off, neutralized with saturated $NaHCO_3$ aqueous solution, washed with water, and dried over anhydrous Na_2SO_4. The solvent was removed by the rotatory evaporator. Recrystallization from CH_2Cl_2–MeOH gave C–H_2P(14B) quantitatively. ^{1}H-NMR ($CDCl_3$): 10.23 (s, 2 H, meso), 8.45 (d, 2 H, J = 7.7 Hz, Ar), 8.20 (d, 3 H, J = 7.7 Hz, Ar), 8.02 (d, 2 H, J = 8.1 Hz, Ar), 7.84 (d, 2 H, J = 8.1 Hz, Ar), 7.23 (d, 1 H, J = 14.5 Hz, Car-H_7′), 7.00 (d, 1 H, J = 14.5 Hz, Car-H_8′), 6.79 (dd, J = 14.5 and 15.1 Hz, 1 H, Car-H_{11}′), 6.70 (m, 3 H, Car), 6.52 (d, 2 H, J = 14.5 Hz, Car), 6.25–6.45 (m, 3 H, Car), 6.2 (m, 3 H, Car), 4.13 (s, 3 H, ester-Me), 3.98 (m, 8 H, 4Hex-1-CH_2), 2.56 (s, 6 H, 2Me), 2.46 (s, 6 H, 2Me), 2.2 (s, 3 H, Car-Me), 2.1–2.2 (m, 8 H, 4Hex-2-CH_2), 2.06 (s, 3 H, Car-Me), 2.03 (m, 2 H, Car-CH_2), 2.00 (s, 3 H, Car-Me), 1.99 (s, 3 H, Car-Me), 1.73 (s, 3 H, Car-Me), 1.7 (m, 8 H, 4Hex-3-CH_2), 1.6 (m, 2 H, Car-CH_2), 1.4–1.5 (m, 10 H, 4Hex-4-CH_2 and Car-CH_2), 1.3–1.4 (m, 8 H, 4Hex-5-CH_2), 1.04 (s, 6 H, 2Car-Me), 0.89 (m, 12 H, 4-Hex-6-Me), –2.40 (br 2 H, NH). HRMS(FAB): found, m/z 1325.948; calcd for $C_{93}H_{121}N_4O_2$, m/z 1325.949 (M^+ + 1).

C–ZnP(13B) (29% yield). ^{1}H-NMR ($CDCl_3$): 10.18 (s, 2 H, meso), 8.45 (d, 2 H, J = 8.6 Hz, Ar), 8.19 (d, 2 H, J = 8.6 Hz, Ar), 8.18 (s, 1 H, Ar), 7.93 (d, 1 H, J = 8.3 Hz, Ar), 7.87 (d, 1 H, J = 8.3 Hz, Ar), 7.70 (t, 1 H, J = 8.3 Hz, Ar), 7.06 (s, 1 H, J = 15.4 Hz, Car-H_7′), 6.85 (d, 1 H, J = 15.4 Hz, Car-H_8′), 6.6 (m, 4 H, Car), 6.35 (d, 2 H, J = 15.0 Hz, Car), 6.30 (d, 1 H, J = 12.0 Hz, Car), 6.2 (m, 2 H, Car), 6.1 (m, 3 H, Car), 4.14 (s, 3 H, ester-Me), 3.95 (m, 8 H, 4Hex-1-CH_2), 2.53 (s, 6 H, 2Me), 2.43 (s, 6 H, 2Me), 2.2 (m, 8 H, 4Hex-2-CH_2), 2.09 (s, 3 H, Car-Me), 2.0 (m, 2 H, Car-CH_2), 1.96 (s, 6 H, 2Car-Me), 1.94 (s, 3 H, Car-Me), 1.7–1.8 (m, 8 H, 4Hex-3-CH_2), 1.71 (s, 3 H, Car-Me), 1.6 (m, 2 H, Car-CH_2), 1.5 (m, 10 H, 4Hex-4-CH_2 and Car-CH_2), 1.4 (m, 8 H, 4Hex-5-CH_2), 1.02 (s, 6 H, 2Car-Me), 0.89 (m, 12H, 4Hex-6-Me). HRMS(FAB): found, m/z 1386.860; calcd for $C_{93}H_{118}N_4O_2Zn$, m/z 1386.855 (M^+).

C–H_2P(13B). ^{1}H-NMR ($CDCl_3$): 10.25 (s, 2 H, meso), 8.45 (d, 2 H, J = 7.5 Hz, Ar), 8.20 (d, 2 H, J = 7.5 Hz, Ar), 8.19 (s, 1 H, Ar), 7.92 (d, 1 H, J = 7.8 Hz, Ar), 7.84 (d, 1 H, J = 7.8 Hz, Ar), 7.69 (t, 1 H, J = 7.8 Hz, Ar), 7.12 (d, 1 H, J = 15.6 Hz, Car-H_7′), 6.84 (d, 1 H, J = 15.6 Hz, Car), 6.64 (m, 4 H, Car), 6.1–6.4 (m, 8 H, Car), 4.13 (s, 3 H, ester-Me), 3.98 (m, 8 H, 4Hex-1-CH_2), 2.55 (s, 6 H, 2Me), 2.46 (s, 6 H, 2Me), 2.2 (m, 8 H, 4Hex-2-CH_2), 2.09 (s, 3 H, Car-Me), 2.0 (m, 2 H, Car-CH_2), 1.96 (s, 6 H, 2Car-Me), 1.94 (s, 3 H, Car-Me), 1.65–1.8 (m, 8 H, 4Hex-3-CH_2), 1.71 (s, 3 H, Car-Me), 1.6 (m, 2 H, Car-CH_2), 1.4–1.5 (m, 10H, 4Hex-4-CH_2 and Car-CH_2), 1.3–1.4 (m, 8 H, 4Hex-5-CH_2), 1.02 (s, 3 H, Car-Me), 1.01 (s, 3 H, Car-Me), 0.8–0.9 (m, 12 H, Hex-6-Me), –2.41 (br, 2 H, NH). HRMS(FAB): found, m/z 1325.946; calcd for $C_{93}H_{121}N_4O_2$ m/z 1325.949 (M^+ + 1).

C–ZnP(26N) (12% yield). ^{1}H-NMR ($CDCl_3$): 10.09 (s, 2 H, meso), 8.35 (m, 3 H, Ar), 8.11 (m, 5 H, Ar), 7.83 (d, 1 H, J = 8.5 Hz, Ar), 7.76 (d, 1 H, J = 8.5 Hz, Ar), 7.08 (d, 1 H, J = 16.2 Hz, Car-H_7′), 6.87 (d, 1 H, J = 16.2 Hz, Car-H_8′), 6.5–6.7 (m, 5 H, Car), 6.15–6.4 (m, 3 H, Car), 6.0–6.1 (m, 4 H, Car), 4.03 (s, 3 H, ester-Me), 3.5 (m, 8 H, 4Hex-1-CH_2), 2.55 (s, 6 H, 2Me), 2.42 (s, 6 H, 2Me), 2.0–2.1 (m, 8 H, 4Hex-2-CH_2), 2.11 (s, 3 H, Car-Me), 1.85–2.0 (m, 2 H, Car-CH_2), 2.03 (s, 3 H, Car-Me), 2.00 (s, 3 H, Car-Me), 1.98 (s, 3 H, Car-Me), 1.6–1.7 (m, 8 H, 4Hex-3-CH_2), 1.73 (s, 3 H, Car-Me), 1.55 (m, 2 H, Car-CH_2), 1.4 (m, 10 H, 4Hex-4-CH_2 and Car-CH_2), 1.3 (m, 8 H, 4Hex-5-CH_2), 0.94 (s, 6 H, 2Car-Me), 0.87 (m, 12 H, 4Hex-6-Me). HRMS(FAB): found: m/z 1386.858; calcd for $C_{97}H_{120}N_4O_2Zn$, m/z 1386.855 (M^+).

C–H_2P(26N). ^{1}H-NMR ($CDCl_3$): 10.25 (s, 2 H, meso), 8.45 (m, 3 H, Ar), 8.2 (m, 5 H, Ar), 7.95 (d, 1 H, J = 8.6 Hz, Ar), 7.90 (d, 1 H, J = 8.6 Hz, Ar), 7.17 (d, 1 H, J = 16.1 Hz, Car-H_7′), 7.00 (d, 1 H, J = 16.1 Hz, Car-H_8′), 6.7 (m, 4 H, Car), 6.5 (m, 1 H, Car), 6.25–6.4 (m, 3 H, Car), 6.1–6.2 (m, 4 H, Car), 4.13 (s, 3 H, ester-Me), 3.49 (m, 8 H, 4Hex-1-CH_2), 2.43 (s, 6 H, 2Me), 2.42 (s, 6 H, 2Me), 2.18 (m, 8 H, 4Hex-2-CH_2), 2.19 (s, 3 H, Car-Me), 2.05 (m, 2 H, Car-CH_2), 2.04 (s, 3 H, Car-Me), 2.00 (s, 3 H, Car-Me), 1.98 (s, 3 H, Car-Me), 1.73 (s, 3 H, Car-Me), 1.7–1.8 (m, 8 H, 4Hex-3-CH_2), 1.4–1.5 (m, 10 H, 4Hex-4-CH_2 and Car-CH_2), 1.3–1.4 (m, 8 H, 4Hex-5-CH_2), 1.05 (s, 6 H, 2Car-Me), 0.9 (m, 12 H, 4Hex-6-Me), –2.40 (br, 2 H, NH). MS(FAB): found, m/z 1438 (M^+ + 1).

C–ZnP(27N). ^{1}H-NMR ($CDCl_3$): 10.17 (s, 2 H, meso), 8.45 (m, 3 H, Ar), 8.1–8.2 (m, 5 H, Ar), 7.95 (s, 1 H, Ar), 7.89 (d, 1 H, J = 7.9 Hz, Ar), 7.12 (d, 1 H, J = 16.6 Hz, Car-H_7′), 6.88 (d, 1 H, J = 16.6 Hz, Car-H_8′), 6.6–6.8 (m, 4 H, Car), 6.45 (m, 2 H, Car), 6.2–6.4 (m, 3 H, Car), 6.1–6.2 (m, 3 H, Car), 4.14 (s, 3 H, ester-Me), 3.92 (m, 8 H, 4Hex-1-CH_2), 2.42 (s, 6 H, 2Me), 2.38 (s, 6 H, 2Me), 2.1–2.2 (m, 8 H, 4Hex-2-CH_2), 2.12 (s, 3 H, Car-Me), 1.9–2.1 (m, 2 H, Car-CH_2), 2.00 (s, 3 H, Car-Me), 1.98 (s, 6 H, 2Car-Me), 1.7–1.8 (m, 8 H, 4Hex-3-CH_2), 1.72 (s, 3 H, Me), 1.63 (m, 2 H, Car-CH_2), 1.5 (m, 10 H, 4Hex-4-CH_2 and Car-CH_2), 1.4 (m, 8 H, 4Hex-5-CH_2), 1.03 (s, 6 H, 2Car-Me), 0.90 (t, 6 H, J = 7.8 Hz, 2Hex-6-Me), 0.88 (t, 6 H, J = 7.8 Hz, 2Hex-6-Me). MS(FAB): found, m/z 1438 (M^+ + 1).

C–H_2P(27N). ^{1}H-NMR ($CDCl_3$): 10.25 (s, 2 H, meso), 8.45 (m, 3 H, Ar), 8.1–8.23 (m, 5 H, Ar), 8.0–7.9 (m, 2 H, Ar), 7.13 (d, 1 H, J = 16.1 Hz, Car-H_7′), 6.99 (d, 1 H, J = 16.1 Hz, Car-H_8′), 6.6–6.7 (m, 4 H, Car), 6.3–6.4 (m, 5 H, Car), 6.1–6.2 (m, 3 H, Car), 4.13 (s, 3 H, ester-Me), 3.98 (m, 8 H, 4Hex-1-CH_2), 2.47 (s, 6 H, 2Me), 2.43 (s, 6 H, 2Me), 2.1–2.2 (m, 8 H, Hex-2-CH_2), 2.12 (s, 3 H, Car-Me), 2.0 (m, 2 H, Car-CH_2), 2.00 (s, 3 H, Car-Me), 1.98 (s, 6 H, 2Car-Me), 1.7–1.8 (m, 8 H, 4Hex-3-CH_2), 1.72 (s, 3 H, Car-Me), 1.6–1.7 (m, 2 H, Car-CH_2), 1.45 (m, 10 H, 4Hex-4-CH_2 and Car-CH_2), 1.35 (m, 8 H, 4Hex-5-CH_2), 1.03 (s, 6 H, 2Car-Me), 0.90 (t, 6 H, J = 7.8 Hz, 2Hex-6-Me), 0.88 (t, J = 7.8 Hz, 2Hex-6-Me), –2.36 (br, 2 H, NH). HRMS(FAB): found, m/z 1375.968; calcd for $C_{97}H_{122}N_4O_2$, m/z 1375.965 (M^+ + 1).

C–ZnP(4P04). ^{1}H-NMR ($CDCl_3$): 10.15 (s, 2 H, meso), 8.44 (d, 2 H, J = 8.1 Hz, Ar), 8.19 (d, 2 H, J = 8.1 Hz, Ar), 8.12 (d, 2 H, J = 8.1 Hz, Ar), 8.02 (d, 2 H, J = 8.1 Hz, Ar), 7.94 (d, 2 H, J = 8.6 Hz, Ar), 7.69 (d, 2 H, J = 8.6 Hz, Ar), 7.09 (d, 1 H, J = 16.2 Hz, Car-H_7′), 6.7 (m, 5 H, Car), 6.46 (d, 2 H, J = 14.7 Hz, Car), 6.39 (d, 1 H, J = 12.8 Hz, Car), 6.34 (m, 1 H, Car), 6.29 (m, 2 H, Car), 6.1–6.2 (m, 3 H, Car), 4.14 (s, 3 H, ester-Me), 3.92 (m, 8 H, 4Hex-1-CH_2), 2.52 (s, 6 H, 2Me), 2.41 (s, 6 H, 2Me), 2.1–2.2 (m, 8 H, 4Hex-2-CH_2), 2.14 (s, 3 H, Car-Me), 2.0 (m, 2 H, Car-CH_2), 2.03 (s, 3 H, Car-Me), 2.00 (s, 3 H, Car-Me), 1.99 (s, 3 H, Car-Me), 1.7–1.8 (m, 8 H, 4Hex-3-CH_2), 1.73 (s, 3 H, Car-Me), 1.6–1.7 (m, 2 H, Car-CH_2), 1.5 (m, 10 H, 4Hex-4-CH_2 and Car-CH_2), 1.4 (m, 8 H, 4Hex-5-CH_2), 1.04 (s, 6 H, 2Me), 0.92 (t, 12 H, J = 7.3 Hz, 4Hex-6-Me). MS(FAB): found, m/z 1463 (M^+)–1468 (M^+ + 5).

C–H_2P(4P04). ^{1}H-NMR ($CDCl_3$): 10.25 (s, 2 H, meso), 8.44 (d, 2 H, J = 8.1 Hz, Ar), 8.22 (d, 2 H, J = 8.1 Hz, Ar), 8.13 (d, 2 H, J = 7.7 Hz, Ar), 8.04 (d, 2 H, J = 7.7 Hz, Ar), 7.95 (d, 2 H, J = 8.1 Hz, Ar), 7.69 (d, 2 H, J = 8.1 Hz, Ar), 7.05 (d, 1 H, J = 15.8 Hz, Car-H_7′), 6.7 (m, 5 H, Car), 6.46 (d, 2 H, J = 15.0 Hz, Car), 6.39 (d, 1 H, J = 15.8 Hz, Car), 6.35 (d, 1 H, J = 12.4 Hz, Car), 6.29 (d, 2 H, J = 10.3 Hz, Car), 6.1–6.2 (m, 3 H, Car), 4.13 (s, 3 H, ester-Me), 3.98 (m, 8 H, 4Hex-1-CH_2), 2.56 (s, 6 H, 2Me), 2.46 (s, 6 H, 2Me), 2.2 (m, 8 H, 4Hex-2-CH_2), 2.14 (s, 3 H, Car-Me), 2.03 (s, 3 H, Car-Me), 2.00 (s, 3 H, Car-Me), 2.0 (m, 2 H, Car-CH_2), 1.98 (s, 3 H, Car-Me), 1.7–1.8 (m, 8 H, 4Hex-3-CH_2), 1.73 (s, 3 H, Car-Me), 1.6–1.7 (m, 2 H, Car-CH_2), 1.5 (m, 10 H, 4Hex-4-CH_2 and Car-CH_2), 1.3–1.4 (m, 8 H, 4Hex-5-

CH_2), 1.04 (s, 6 H, 2Car-Me), 0.9 (t, 12 H, J = 7.8 Hz, 4Hex-6-Me), –2.3 (br, 2 H, NH). HRMS(FAB): found, m/z 1401.984; calcd for $C_{99}H_{124}NO_4O_2$, m/z 1401.989 ($M^+ + 1$).

C–ZnP(3P04). ^{1}H-NMR ($CDCl_3$): 10.17 (s, 2 H, meso), 8.43 (d, 2 H, J = 7.8 Hz, Ar), 8.19 (d, 2 H, J = 7.8 Hz, Ar), 8.14 (d, 2 H, J = 7.8 Hz, Ar), 8.05 (d, 2 H, J = 7.8 Hz, Ar), 8.04 (m, 1 H, Ar), 7.70 (m, 1 H, Ar), 7.57 (m, 2 H, Ar), 7.11 (d, 1 H, J = 16.1 Hz, Car-$H_{7'}$), 6.82 (d, 1 H, J = 16.1 Hz, Car-$H_{8'}$), 6.6–6.7 (m, 4 H, Car), 6.48 (d, 2 H, J = 14.6 Hz, Car), 6.2–6.4 (m, 3 H, Car), 4.14 (s, 3 H, ester-Me), 3.95 (m, 8 H, 4Hex-1-CH_2), 2.54 (s, 6 H, 2Me), 2.42 (s, 6 H, 2Me), 2.17 (m, 8 H, 4Hex-2-CH_2), 2.15 (s, 3 H, Car-Me), 2.02 (s, 3 H, Car-Me), 2.0 (m, 2 H, Car-CH_2), 1.98 (s, 3 H, Car-Me), 1.7–1.8 (m, 8 H, 4Hex-3-CH_2), 1.72 (s, 3 H, Car-Me), 1.6 (m, 2 H, Car-CH_2), 1.5 (m, 10 H, 4Hex-4-CH_2 and Car-CH_2), 1.4 (m, 8 H, 4Hex-5-CH_2), 1.04 (s, 6 H, 2Car-Me), 0.9 (t, 12 H, J = 7.8 Hz, 4Hex-6-Me). MS(FAB): found, m/z 1463 (M^+)–1468 ($M^+ + 5$).

C–H_2P(3P04). ^{1}H-NMR ($CDCl_3$): 10.25 (s, 2 H, meso), 8.43 (d, 2 H, J = 7.8 Hz, Ar), 8.19 (d, 2 H, J = 7.8 Hz, Ar), 8.14 (d, 2 H, J = 8.3 Hz, Ar), 8.02 (d, 2 H, J = 8.3 Hz, Ar), 8.00 (s, 1 H, Ar), 7.81 (m, 1 H, Ar), 7.56 (m, 2 H, Ar), 7.11 (d, 1 H, J = 16.1 Hz, Car-$H_{7'}$), 6.82 (d, 1 H, J = 16.1 Hz, Car-$H_{8'}$), 6.6–6.7 (m, 4 H, Car), 6.45 (d, 2 H, J = 14.7 Hz, Car), 6.2–6.4 (m, 3 H, Car), 6.1–6.2 (m, 3 H, Car), 4.14 (s, 3 H, ester-Me), 3.98 (m, 8 H, 4Hex-1-CH_2), 2.57 (s, 6 H, 2Me), 2.47 (s, 6 H, 2Me), 2.1–2.2 (m, 8 H, 4Hex-2-CH_2), 2.14 (s, 3 H, Car-Me), 2.02 (s, 3 H, Car-Me), 2.0 (m, 2 H, Car-CH_2), 1.98 (s, 3 H, Car-Me), 1.97 (s, 3 H, Car-Me), 1.7–1.8 (m, 8 H, 4Hex-3-CH_2), 1.72 (s, 23 H, Car-Me), 1.6 (m, 2 H, Car-CH_2), 1.45 (m, 10 H, 4Hex-4-CH_2 and Car-CH_2), 1.35 (m, 8 H, 4Hex-5-CH_2), 1.03 (s, 6 H, 2Car-Me), 0.90 (t, 12 H, J = 7.8 Hz, 4Hex-6-Me), –2.30 (br, 2 H, NH). HRMS(FAB): found, m/z 1401.984; calcd for $C_{99}H_{124}N_4O_2$, m/z 1401.989 ($M^+ + 1$).

C–ZnP(4P03). ^{1}H-NMR ($CDCl_3$): 10.16 (s, 2 H, meso), 8.43 (d, 2 H, J = 7.3 Hz, Ar), 8.40 (m, 1 H, Ar), 8.20 (d, 2 H, J = 7.3 Hz, Ar), 8.06 (dd, 1 H, J = 6.0 and 8.2 Hz, Ar), 7.82 (d, 2 H, J = 7.8 Hz, Ar), 7.80 (m, 1 H, Ar), 7.52 (d, 2 H, J = 7.8 Hz, Ar), 6.95 (d, 1 H, J = 16.1 Hz, Car-$H_{7'}$), 6.6–6.7 (m, 5 H, Car), 6.1–6.5 (m, 8 H, Car), 4.14 (s, 3 H, ester-Me), 3.92 (m, 8 H, 4Hex-1-CH_2), 2.54 (s, 6 H, 2Me), 2.42 (s, 6 H, 2Me), 2.1 (m, 8 H, 4Hex-2-CH_2), 2.0–2.1 (m, 14 H, CH_2 and 4Car-Me), 1.7–1.8 (m, 11 H, 4Hex-3-CH_2 and Car-Me), 1.62 (m, 2 H, Car-CH_2), 1.5 (m, 10 H, 4Hex-4-CH_2 and Car-CH_2), 1.4 (m, 8 H, 4Hex-5-CH_2), 1.33 (m, 2 H, Car-CH_2), 1.04 (s, 6 H, 2Me), 0.9 (t, 6 H, J = 7.3 Hz, 2Hex-6-Me), 0.89 (t, 6 H, J = 7.3 Hz, 2Hex-6-Me). MS(FAB): found; m/z 1465 ($M^+ + 2$).

C–H_2P(4P03). ^{1}H-NMR ($CDCl_3$): 10.25 (s, 2 H, meso), 8.45 (d, 2 H, J = 7.8 Hz, Ar), 8.40 (m, 1 H, Ar), 8.2 (d, 2 H, J = 7.8 Hz, Ar), 8.05 (dd, 1 H, J = 6.4 and 7.8 Hz, Ar), 7.82 (m, 1 H, Ar), 7.80 (d, 2 H, J = 7.8 Hz, Ar), 7.60 (m, 1 H, Ar), 7.55 (d, 1 H, J = 7.8 Hz, Ar), 7.00 (d, 1 H, J = 15.1 Hz, Car-$H_{7'}$), 6.6–6.7 (m, 5 H, Car), 6.1–6.5 (m, 8 H, Car), 4.13 (s, 3 H, ester-Me), 3.98 (m, 8 H, 4Hex-1-CH_2), 2.56 (s, 6 H, 2Me), 2.47 (s, 6 H, 2Me), 2.2 (m, 8 H, 4Hex-2-CH_2), 2.0 (m, 14 H, Car-CH_2 and 4Car-Me), 1.75 (m, 11 H, 4Hex-3-CH_2 and Car-Me), 1.6 (m, 2 H, Car-CH_2), 1.5 (m, 10 H, 4Hex-4-CH_2 and Car-CH_2), 1.35 (m, 8 H, 4Hex-5-CH_2), 1.03 (s, 6 H, 2Car-Me), 0.0 (t, 12 H, J = 7.6 Hz, 4Hex-6-Me), –2.37 (br, 2 H, NH). HRMS(FAB): found, m/z 1401.992; calcd for $C_{99}H_{124}N_4O_2$, m/z 1401.989 ($M^+ + 1$).

C–ZnP(P1). ^{1}H-NMR ($CDCl_3$): 10.11 (s, 2 H, meso), 8.4 (d, 2 H, J = 8.12 Hz, Ar), 8.19 (d, 2 H, J = 8.12 Hz, Ar), 7.99 (d, 2 H, J = 7.69 Hz, Ar), 7.56 (d, 4 H, Ar), 7.42 (d, 2 H, J = 8.12 Hz, Ar), 7.01 (d, 1 H, J = 15.82 Hz, Car), 6.7 (m, 5 H, Car), 6.1–6.5 (d, 8 H, Car), 4.36 (s, 2 H, CH_2), 4.14 (s, 3 H, Me), 3.9 (m, 8 H, 4Hex-1-CH_2), 2.47 (s, 6 H, 2Me), 2.40 (s, 6 H, 2Me), 2.1–2.2 (m, 11 H, 4Hex-2-CH_2 and Me), 2.0 (m, 11 H, Car-CH_2 and 3Car-Me), 1.7–.18 (m, 11 H, 4Hex-3-CH_2 and Car-Me), 1.6–1.7 (m, 2 H, Car-CH_2), 1.5 (m, 10 H, 4Hex-4-CH_2 and Car-Me), 1.4 (m, 8 H, 4Hex-5-CH_2), 1.05 (s, 6 H, 2Me), 0.9 (m, 12 H, 4Hex-6-Me). MS(FAB): m/z 1478 ($M^+ + 1$).

C–H_2P(P1). ^{1}H-NMR ($CDCl_3$): 10.23 (s, 2 H, meso), 8.44 (d, 2 H, J = 8.1 Hz, Ar), 8.20 (d, 2 H, J = 8.1 Hz, Ar), 7.99 (d, 2 H, J = 7.7 Hz, Ar), 7.58 (d, 2 H, J = 7.7 Hz, Ar), 7.54 (d, 2 H, J = 8.1 Hz, Ar), 7.41 (d, 2 H, J = 8.1 Hz, Ar), 6.96 (d, 1 H, J = 15.8 Hz, Car-$H_{7'}$), 6.6–6.7 (m, 5 H, Car), 6.2–6.5 (m, 5 H, Car), 6.1–6.2 (m, 3 H, Car), 4.34 (s, 3 H, ester-Me), 3.97 (m, 8 H, 4Hex-1-CH_2), 2.51 (s, 6 H, 2Me), 2.45 (s, 6 H, 2Me), 2.17 (m, 8 H, 4Hex-2-CH_2), 2.09 (s, 3 H, Me), 2.01 (s, 3 H, Car-Me), 2.00 (m, 2 H, Car-CH_2), 1.99 (s, 3 H, Car-Me), 1.98 (s, 3 H, Car-Me), 1.7–1.8 (m, 8 H, 4Hex-3-CH_2), 1.72 (s, 3 H, Cat-Me), 1.6 (m, 2 H, Car-CH_2), 1.45 (m, 10 H, 4Hex-4-CH_2 and Car-CH_2), 1.35 (m, 8 H, 4Hex-5-CH_2), 1.03 (s, 6 H, 2Car-Me), 0.90 (t, 6 H, J = 7.8 Hz, 2Hex-6-Me), 0.89 (t, 6 H, J = 7.8 Hz, 2Hex-6-Me), –2.41 (br, 2 H, NH). MS(FAB): found, m/z 1415.998; calcd for $C_{100}H_{126}N_4O_2$, m/z 1415.996 ($M^+ + 1$).

C–ZnP(1S5). ^{1}H-NMR ($CDCl_3$): 10.20 (s, 1 H, meso), 10.18 (s, 1 H, meso), 8.42 (d, 2 H, J = 8.1 Hz, Ar), 8.21 (d, 1 H, J = 8.1 Hz, Ar), 8.20 (d, 1 H, J = 8.1 Hz, Ar), 7.91 (s, 1 H, Ar), 7.82 (d, 1 H, J = 7.8 Hz, Ar), 7.45 (d, 1 H, J = 7.8 Hz, Ar), 7.17 (d, 1 H, J = 7.1 Hz, Ar), 7.05 (d, 1 H, J = 7.1 Hz, Ar), 6.98 (d, 1 H, J = 15.8 Hz, Car-$H_{7'}$), 6.6–6.8 (m, 5 H, Car), 6.1–6.5 (d, 8 H, Car), 4.13 (s, 3 H, ester-Me), 3.98 (m, 8 H, 4Hex-1-CH_2), 2.6–2.7 (m, 3 H, CH_2), 2.56 (s and m, 4 H, Me and CH_2), 2.53 (s, 3 H, Me), 2.43 (s, 6 H, 2Me), 2.2 (m, 10 H, 4Hex-2-CH_2 and Car-CH_2), 2.10 (s, 3 H, Car-Me), 2.0 (m, 11 H, CH_2 and 3Car-Me), 1.7–1.8 (m, 11 H, 4Hex-3-CH_2 and Car-Me), 1.61 (s, 3 H, Me), 1.58 (s, 3 H, Me), 1.56 (s, 6 H, 2Me), 1.3–1.5 (m, 18 H, 4Hex-4-CH_2, 4Hex-5-CH_2, and Car-CH_2), 1.05 (s, 6 H, 2Car-Me), 0.89 (t, 6 H, J = 7.8 Hz, 2Hex-6-Me), 0.88 (t, 6 H, J = 7.8 Hz, 2Hex-6-Me). MS(FAB): found, m/z 1587 ($M^+ + 1$).

C–H_2P(1S5). ^{1}H-NMR ($CDCl_3$): 10.25 (s, 1 H, meso), 10.26 (s, 1 H, meso), 8.43 (d, 2 H, J = 7.8 Hz, Ar), 8.20 (d, 2 H, J = 7.8 Hz, Ar), 7.90 (s, 1 H, Ar), 7.80 (m, 1 H, Ar), 7.45 (m, 1 H, Ar), 7.37 (m, 1 H, Ar), 7.18 (d, 1 H, J = 7.3 Hz, Ar), 7.04 (d, 1 H, J = 7.3 Hz, Ar), 7.01 (d, 1 H, J = 15.8 Hz, Ca-$H_{7'}$), 6.6–6.75 (m, 5 H, Car), 6.1–6.5 (m, 8 H, Car), 4.13 (s, 3 H, ester-Me), 3.97 (m, 8 H, 4Hex-1-CH_2), 2.65 (s, 6 H, 2Me), 2.57 (s, 3 H, Me), 2.56 (s and m, 5 H, Me and CH_2), 2.46 (s, 6 H, 2Me), 2.2 (m, 8 H, 4Hex-2-CH_2), 2.10 (s, 3 H, Car-Me), 2.0 (m, 11 H, Car-CH_2 and 3Car-Me), 1.75 (m, 11 H, 4Hex-3-CH_2 and Car-Me), 1.60 (s and m, 5 H, Me and Car-CH_2), 1.58 (s, 3 H, Me), 1.5 (m, 10 H, 4Hex-4-CH_2 and Car-CH_2), 1.4 (m, 8 H, 4Hex-5-CH_2), 1.04 (s, 6 H, 2Car-Me), 0.0 (m, 12 H, 4Hex-6-Me), –2.40 (br, 2 H, NH). HRMS(FAB): found, m/z 1524.090; calcd for $C_{108}H_{138}N_4O_2$, m/z 1524.091 ($M^+ + 1$).

C–ZnP(1S6). ^{1}H-NMR ($CDCl_3$): 10.15 (s, 1 H, meso), 10.11 (s, 1 H, meso), 8.43 (d, 2 H, J = 8.4 Hz, Ar), 8.19 (d, 1 H, J = 8.4 Hz, Ar), 8.17 (d, 1 H, J = 8.4 Hz, Ar), 7.86 (dd, 1 H, J = 1.5 and 7.8 Hz, Ar), 7.58 (s, 1 H, Ar), 7.56 (d, 1 H, J = 7.8 Hz, Ar), 7.13 (d, 1 H, J = 7.8 Hz, Ar), 7.0 (m, 1 H, Ar), 6.91 (d, 1 H, J = 16.1 Hz, Car-$H_{7'}$), 6.75 (m, 1 H, Car), 6.4–6.7 (m, 6 H, Car), 6.0–6.4 (m, 6 H, Car), 4.12 (s, 3 H, ester-Me), 3.9 (m, 8 H, 4Hex-1-CH_2), 2.5–2.7 (m, 4 H, $2CH_2$), 2.60 (s, 3 H, Me), 2.47 (s, 3 H, Me), 2.41 (s, 3 H, Me), 2.40 (s, 3 H, Me), 1.9–2.2 (m, 22 H, 4Hex-2-CH_2, Car-CH_2, and 4Car-Me), 1.6–1.8 (m, 25 H, 4Hex-3-CH_2, Car-CH_2, and 5Me), 1.3–1.5 (m, 18 H, 4Hex-4-CH_2, 4Hex-5-CH_2, and Car-CH_2), 1.04 9s, 6 H, 2Car-Me), 0.8–0.9 (m, 12 H, 4Hex-6-Me). MS(FAB): found, m/z 1587 ($M^+ + 1$).

C–H_2P(1S6). ^{1}H-NMR ($CDCl_3$): 10.20 (s, 1 H, meso), 10.16 (s, 1 H, meso), 8.41 (d, 1 H, J = 8.4 Hz, Ar), 8.18 (d, 1 H, J = 8.4 Hz, Ar), 8.16 (d, 1 H, J = 8.4 Hz, Ar), 7.82 (d, 1 H, J = 7.8 Hz, Ar), 7.59 (s, 1 H, Ar), 7.55 (d, 1 H, J = 7.8 Hz, Ar), 7.25 (s, 1 H, Ar), 7.15 (d, 1 H, J = 7.8 Hz, Ar), 7.02 (d, 1 H, J = 7.8 Hz, Ar), 6.91 (d, 1 H, J = 16.1 Hz, Car-$H_{7'}$), 6.65 (m, 1 H, Car), 6.4–6.7 (m, 6 H, Car), 6.25–6.4 (m, 3 H, Car), 6.1–6.2 (m, 3 H, Car), 4.12 (s, 3 H, ester-Me), 3.95 (m, 8 H, 4Hex-1-CH_2), 2.4–2.6 (m, 8 H, 4Hex-2-CH_2), 2.61 (s, 3 H, Me), 2.50 (s, 3 H, Me), 2.44 (s, 3 H, Me), 2.43 (s, 3 H, Me), 2.15 and 2.03 (ABq, J = 13.0 Hz, $2CH_2$), 1.9–2.0 (m, 2 H, Car-CH_2), 1.98 (s, 3 H, Car-Me), 1.97 (s, 3 H, Car-Me), 1.75 (s, 3 H, Car-Me), 1.72 (s, 3 H, Car-Me), 1.66 (s, 3 H, Car-Me), 1.6–1.8 (m, 20 H, 4Hex-3-CH_2 and 4Me), 1.3–1.5 (m, 18 H, 4Hex-4-CH_2, 4Hex-5-CH_2, and Car-CH_2), 1.04 (s, 6 H, 2Car-Me), 0.8–0.9 (m, 12 H, 4hex-6-Me), –2.47 (br, 2 H, NH). HRMS(FAB): found; m/z 1524.094; calcd for $C_{108}H_{138}N_4O_2$, m/z 1524.091 ($M^+ + 1$).

C–H_2P–Im(14B). ^{1}H-NMR ($CDCl_3$): 10.21 (s, 2 H, meso), 8.31 (s, 2 H, Im-Ar), 8.03 (d, 2 H, J = 7.3 Hz, Ar), 8.00 (d, 2 H, J = 7.8 Hz, Ar), 7.83 (d, 2 H, J = 7.3 Hz, Ar), 7.74 (d, 2 H, J = 7.8 Hz, Ar), 7.22 (d, 1 H, Car), 6.96 (d, 1 H, J = 16.1 Hz, Car), 6.6–6.8 (m, 4 H, Car), 6.56 (d, 2 H, J = 16.1 Hz, Car), 6.3–6.4 (m, 3 H, Car), 6.1–6.2 (m, 3 H, Car), 5.24 (s, 2 H, Im–CH_2–Ar), 3.95 (m, 8 H, 4Hex-1-CH_2), 3.76 (t, 2 H, J = 7.3 Hz, Im–Hex–1–CH_2), 2.55 (s, 6 H, 2Me), 2.41 (s, 6 H, 2Me), 2.22 (s, 3 H, Car–Me), 2.15 (m, 8 H, 4Hex-2-CH_2), 1.9–2.1 (m, 2 H, Car-CH_2), 2.02 (s, 3 H, Car-Me), 1.99 (s, 3 H, Car-Me), 1.89 (s, 3 H, Car-Me), 1.7 (m, 11 H, 4Hex-3-CH_2 and Car-Me), 1.62 (m, 2 H, Im-Hex-2-CH_2), 1.5 (m, 2 H, Car-CH_2), 1.4–1.5 (m, 12 H, 4Hex-4-CH_2, Im-Hex-3-CH_2, and Car-CH_2), 1.3–1.4 (m, 12 H, 4Hex-5-CH_2, Im-Hex-4-CH_2, and Im-Hex-5-CH_2), 1.04 (s, 6 H, 2Car-Me), 0.9 (m, 15 H, 4Hex-6-Me and Im-Hex-6-Me), –2.40 (br, 2 H, NH). HRMS-(FAB): found, m/z 1580.037; calcd for $C_{108}H_{135}N_6O_4$, m/z 1580.054 ($M^+ + 1$).

C–H_2P–Im(P1). ^{1}H-NMR ($CDCl_3$): 10.20 (s, 2 H, meso), 8.29 (s, 2 H, Im-Ar), 8.04 (d, 2 H, J = 7.7 Hz, Ar), 8.00 (d, 2 H, J = 7.3 Hz, Ar), 7.73 (d, 2 H, J = 8.1 Hz, Ar), 7.57 (d, 2 H, J = 7.7 Hz, Ar), 7.52

(d, 2 H, J = 7.3 Hz, Ar), 7.41 (d, 2 H, J = 8.1 Hz, Ar), 7.00 (d, 1 H, J = 14.5 Hz, Car-H$_7$'), 6.5–6.7 (m, 5 H, Car), 6.1–6.5 (m, 8 H, Car), 5.23 (s, 2 H, Im-CH$_2$-Ar), 4.34 (s, 2 H, Ar-CH$_2$-Ar), 3.97 (m, 8 H, 4Hex-1-CH$_2$), 3.75 (t, 2 H, J = 7.3 Hz, Im-Hex-1-CH$_2$), 2.52 (s, 6 H, 2Me), 2.41 (s, 6 H, 2Me), 2.17 (m, 8 H, 4Hex-2-CH$_2$), 2.10 (s, 3 H, Car-Me), 2.01 (s, 3 H, Car-Me), 2.0 (m, 2 H, Car-CH$_2$), 1.99 (s, 3 H, Car-Me), 1.98 (s, 3 H, Car-Me), 1.73 (s, 3 H, Car-Me), 1.6–1.7 (m, 10 H, 4Hex-3-CH$_2$ and Im-Hex-2-CH$_2$), 1.6 (m, 2 H, Car-CH$_2$), 1.5 (m, 12 H, 4Hex-4-CH$_2$, Im-Hex-3-CH$_2$, and Car-CH$_2$), 1.4 (m, 12 H, 4Hex-5-CH$_2$, Im-Hex-4-CH$_2$, and Im-Hex-5-CH$_2$), 1.04 (s, 6 H, 2Car-Me), 0.91 (m, 15 H, 4Hex-6-Me and Im-Hex-6-Me), –2.4 (br, 2 H, NH). HRMS(FAB): found, m/z 1670.107; calcd for $C_{115}H_{141}N_6O_4$, m/z 1670.111 (M$^+$ + 1).

Synthesis of C–H$_2$P(Am), C–ZnP(Am), and C–H$_2$P–Im(Am). 5-(4-(Acetylamino)phenyl)-15-(4-methylphenyl)-2,8-12,18-tetrahexyl-3,7,13,17-tetramethylporphine (**13**) was prepared from 4-(acetylamino)benzaldehyde (64 mg, 0.4 mmol), 4-methylbenzaldehyde (48 mg, 0.4 mmol), and **1** (0.8 mmol, 264 mg) in dry CH$_3$CN via the same method described for C-H$_2$P(14B). The yield of **13** was 100 mg (0.11 mmol, 25% yield). ^{1}H-NMR (CDCl$_3$): 10.23 (s, 2 H, meso), 7.98 (d, 2 H, J = 8.1 Hz, Ar), 7.94 (d, 2 H, J = 7.7 Hz, Ar), 7.83 (d, 2 H, J = 8.1 Hz, Ar), 7.55 (d, 2 H, J = 7.7 Hz, Ar), 7.44 (s, 1 H, N*H*CO), 3.98 (m, 8 H, 4Hex-1-C*H*$_2$), 2.74 (s, 3 H, Ar-*Me*), 2.52 (s, 12 H, 4Me), 2.32 (s, 3 H, *Me*CO), 2.17 (m, 8 H, 4Hex-2-CH$_2$), 1.74 (m, 8 H, 4Hex-3-C*H*$_2$), 1.49 (m, 8 H, 4Hex-4-C*H*$_2$), 1.40 (m, 8 H, 4Hex-5-C*H*$_2$), 0.92 (t, 12 H, J = 7.3 Hz, 4Hex-6-*Me*), –2.42 (br 2 H, NH). HRMS(FAB): found, m/z 926.676; calcd for $C_{63}H_{84}N_5O$, m/z 926.673 (M$^+$ + 1). Anal. Calcd for $C_{63}H_{83}N_5O$: C, 81.68; H, 9.03; N, 7.56. Found: C, 81.73; H, 9.00; N, 7.62.

5-(4-Aminophenyl)-15-(4-methylphenyl)-2,8-12,18-tetrahexyl-3,7,13,17-tetramethylporphine (**14**). The porphyrin **13** (43 mg, 47 μmol) was dissolved in a mixture of EtOH (10 mL) and 1 N HCl (20 mL), and the resulting solution was heated to reflux for 3 h under a nitrogen atmosphere. The solution was cooled to room temperature, neutralized with a saturated NaHCO$_3$ aqueous solution, and extracted with CH$_2$Cl$_2$ until colorless. The CH$_2$Cl$_2$ layers were combined, washed with water, and dried over anhydrous Na$_2$SO$_4$. The solvent was removed by the rotary evaporator. Recrystallization from CH$_2$Cl$_2$–MeOH gave **14** (20 mg, 20 μmol, 51% yield). ^{1}H-NMR (CDCl$_3$): 10.21 (s, 2 H, meso), 7.93 (d, 2 H, J = 7.9 Hz, Ar), 7.79 (d, 2 H, J = 8.1 Hz, Ar), 7.53 (d, 2 H, J = 7.9 Hz, Ar), 7.06 (d, 2 H, J = 8.1 Hz, Ar), 3.97 (m, 8 H, 4Hex-1-C*H*$_2$), 2.72 (s, 3 H, Ar-*Me*), 2.61 (s, 6 H, 2Me), 2.51 (s, 6 H, 2Me), 2.18 (m, 8 H, 4Hex-2-C*H*$_2$), 1.73 (m, 8 H, 4Hex-3-C*H*$_2$), 1.47 (m, 8 H, 4Hex-4-C*H*$_2$), 1.37 (m, 8 H, 4Hex-5-C*H*$_2$), 0.89 (t, 12 H, J = 7.3 Hz, 4Hex-6-*Me*), –2.42 (br, 2 H, NH). HRMS(FAB): found, m/z 884.666; calcd for $C_{61}H_{82}N_5$, m/z 884.663 (M$^+$ + 1). Anal. Calcd for $C_{61}H_{81}N_5$: C, 82.85; H, 9.23; N, 7.92. Found: C, 82.82; H, 9.26; N, 7.90.

To a solution of 7'-apo-7'-(4-carboxyphenyl)-β-carotene (**9**)[23e] (60 mg, 0.11 mmol and CDMT (15 mg, 90 mmol) in dry CH$_2$Cl$_2$ (30 mL) was added 4-methylmorpholine (11 mg, 0.11 mmol) at 0 °C under a nitrogen atmosphere. After being stirred for 1 h, the porphyrin **14** (15 mg, 17 μmol) and *N*-methylmorpholine (11 mg, 0.11 mmol) were added to the above solution at 0 °C and the resulting mixture was stirred for an additional 14 h at room temperature. Then the solution was washed with 1 N HCl, saturated NaHCO$_3$ aqueous solutions, and brine, and the organic layer was separated off, washed with water, and dried over anhydrous Na$_2$SO$_4$. The solvent was removed by the rotary evaporator. Purification by flash column chromatography (silica gel, CH$_2$Cl$_2$) and recrystallization from CH$_2$Cl$_2$–MeOH gave C-H$_2$P(Am) (8 mg, 4.5 μmol, 56% yield). ^{1}H-NMR (CDCl$_3$): 10.23 (s, 2 H, meso), 8.18 (s, 1 H, N*H*CO), 8.07 (m, 4 H, Car-Ar), 8.01 (d, 2 H, J = 8.1 Hz, Ar), 7.92 (d, 2 H, J = 7.7 Hz, Ar), 7.65 (d, 2 H, J = 8.1 Hz, Ar), 7.55 (d, 2 H, J = 7.7 Hz, Ar), 7.06 (d, 1 H, J = 15.8 Hz, Car-H$_7$'), 6.65–6.75 (m, 5 H, Car), 6.3–6.5 (m, 5 H, Car), 6.2 (m, 3 H, Car), 3.98 (m, 8 H, 4Hex-1-CH$_2$), 2.72 (s, 3 H, Ar-Me), 2.57 (s, 6 H, 2Me), 2.51 (s, 6 H, 2Me), 2.2 (m, 8 H, 4Hex-2-CH$_2$), 2.11 (s, 3 H, Car-Me), 2.02 (s, 3 H, Car-Me), 2.00 (s, 3 H, Car-Me), 1.99 (s, 3 H, Car-Me), 2.02–2.1 (m, 2 H, Car-CH$_2$), 1.8 (m, 8 H, 4Hex-3-CH$_2$), 1.73 (s, 3 H, Car-Me), 1.6–1.7 (m, 10 H, 4Hex-3-CH$_2$ and Im-Hex-2-CH$_2$), 1.6 (m, 2 H, Car-CH$_2$), 1.4–1.5 (m, 8 H, 4Hex-4-CH$_2$), 1.3–1.4 (m, 10 H, 4Hex-5-CH$_2$ and Im-Hex-3-CH$_2$), 1.25 (m, 12 H, 4Hex-5-CH$_2$, Im-Hex-4-CH$_2$, and Im-Hex-5-CH$_2$), 1.16 (m, 2 H, Car-CH$_2$), 1.04 (s, 6 H, 2Car-Me), 0.90 (t, 12 H, 4Hex-6-Me), –2.38 (br, 2 H, NH). HRMS(FAB): found, m/z 1400.995; calcd for $C_{99}H_{126}N_5O$, m/z 1400.997 (M$^+$ + 1).

C–ZnP(Am) was obtained in quantitative yield from C–H$_2$P(Am) upon treatment with Zn(OAc)$_2$. ^{1}H-NMR (CDCl$_3$): 10.19 (s, 2 H, meso), 8.19 (s, 1 H, N*H*CO), 8.05–8.10 (m, 4 H, Car-Ar), 8.02 (d, 2 H, J = 8.6 Hz, Ar), 7.93 (d, 2 H, J = 7.7 Hz, Ar), 7.65 (d, 2 H, J = 8.6 Hz, Ar), 7.55 (d, 2 H, J = 7.7 Hz, Ar), 7.06 (d, 1 H, J = 16.2 Hz, Car-H$_7$'), 6.6–6.8 (m, 5 H, Car), 6.3–6.5 (d, 5 H, Car), 6.2 (m, 3 H, Car), 3.97 (m, 8 H, 4Hex-1-C*H*$_2$), 2.73 (s, 3 H, Ar-*Me*), 2.55 (s, 6 H, 2Me), 2.48 (s, 6 H, 2Me), 2.2 (m, 8 H, 4Hex-2-C*H*$_2$), 2.11 (s, 3 H, Car-Me), 2.02 (s, 3 H, Car-Me), 2.00 (s, 3 H, Car-Me), 1.98 (s, 3 H, Car-Me), 1.9–2.0 (m, 2 H, Car-CH$_2$), 1.7–1.8 (m, 8 H, 4Hex-3-CH$_2$), 1.73 (s, 3 H, Car-Me), 1.6 (m, 2 H, Car-CH$_2$), 1.5 (m, 10 H, 4Hex-4-CH$_2$ and Car-CH$_2$), 1.4 (m, 8 H, 4Hex-5-CH$_2$), 1.3–1.2 (m, 2 H, Car-CH$_2$), 1.04 (s, 6 H, 2Car-Me), 0.91 (t, 12 H, J = 7.3 Hz, 4Hex-6-Me). MS(FAB): found, m/z 1462 (M$^+$).

The porphyrin **15** was synthesized by the condensation reaction of **3** (100 mg, 0.24 mmol) and 4-(acetylamino)benzaldehyde (163 mg, 1 mmol) with **1** (413 mg, 1.25 mmol) in the same manner as described for **13**. Yield: 80 mg, 26%. ^{1}H-NMR (CDCl$_3$): 10.17 (s, 2 H, meso), 8.02 (d, 2 H, J = 7.9 Hz, Ar), 8.00 (d, 2 H, J = 7.9 Hz, Ar), 7.89 (s, 2 H, Im-Ar), 7.86 (d, J = 7.9 Hz, Ar), 7.68 (d, J = 7.9 Hz, Ar), 7.49 (s, 1 H, N*H*CO), 5.08 (s, 2 H, Im-C*H*$_2$-Ar), 3.93 (m, 8 H, 4Hex-1-C*H*$_2$), 3.65 (t, 2 H, J = 7.7 Hz, Im-1-C*H*$_2$), 2.49 (s, 6 H, 2Me), 2.38 (s, 6 H, 2Me), 2.37 (s, 3 H, *Me*CO), 2.14 (m, 8 H, 4Hex-2-C*H*$_2$), 1.73 (m, 10 H, 4Hex-3-C*H*$_2$ and Im-Hex-2-C*H*$_2$), 1.5 (m, 10 H, 4Hex-4-CH$_2$ and Im-Hex-3-C*H*$_2$), 1.4 (m, 12 H, 4Hex-5-C*H*$_2$, Im-4-C*H*$_2$, and Im-Hex-5-C*H*$_2$), 0.90 (m, 15 H, 4Hex-6-Me and Im-Hex-6-Me), –2.60 (br, 2 H, NH). HRMS(FAB): found, m/z 1224.765; calcd for $C_{77}H_{98}N_7O_5$, m/z 1224.770 (M$^+$ + 1). Anal. Calcd for $C_{79}H_{97}N_7O_5$: C, 77.48; H, 7.98; N, 8.01. Found: C, 77.55; H, 8.02; N, 7.96.

The porphyrin **16** was synthesized in the same manner as described for **14** (80 mg, 62 μmol, 6 N HCl (15 mL), ethanol (10 mL), refluxed for 3 h). Yield: 50 mg, 68%. ^{1}H-NMR (CDCl$_3$): 10.16 (s, 2 H, meso), 8.03 (d, 2 H, J = 7.9 Hz, Ar), 7.82 (d, J = 7.9 Hz, Ar), 7.72 (s, 2 H, Im-Ar), 7.65 (d, 2 H, J = 7.9 Hz, Ar), 7.07 (d, 2 H, J = 7.9 Hz, Ar), 5.01 (s, 2 H, Im-C*H*$_2$-Ar), 4.0 (m, 8 H, 4Hex-1-C*H*$_2$), 3.61 (t, 2 H, J = 7.3 Hz, Im-Hex-1-C*H*$_2$), 2.62 (s, 6 H, 2Me), 2.41 (s, 6 H, 2Me), 2.1–2.2 (m, 8 H, 4Hex-2-C*H*$_2$), 1.7–1.8 (m, 10 H, 4Hex-3-C*H*$_2$ and Im-Hex-2-C*H*$_2$), 1.47 (m, 10 H, 4Hex-4-C*H*$_2$ and Im-Hex-3-C*H*$_2$), 1.37 (m, 12 H, 4Hex-5-CH$_2$, Im-Hex-4-C*H*$_2$, and Im-Hex-5-C*H*$_2$), 0.90 (m, 15 H, 4Hex-6-Me and Im-6-Me), –2.60 (br, 2 H, NH). HRMS(FAB): found, m/z 1182.754; calcd for $C_{77}H_{96}N_7O_4$, m/z 1182.759 (M$^+$ + 1). Anal. Calcd for $C_{77}H_{95}N_7O_4$: C, 78.20; H, 8.10; N, 5.41. Found: C, 78.25; H, 8.04; N, 5.38.

The porphyrin C–H$_2$P–Im(Am) was synthesized in the same manner as the synthesis of C–H$_2$P(Am) from **9** (25 mg, 47 μmol), CDMT (19.2 mg, 101 μmol), 4-methylmorpholine (10 μL, 215 μmol), and **16** (10 mg, 8 mmol). Yield: 8 mg, 57%. ^{1}H-NMR (CDCl$_3$): 10.11 (s, 2 H, meso), 8.22 (s, 2 H, Im-Ar), 8.08 (s, 1 H, N*H*CO), 7.97 (m, 4 H, Car-Ar), 7.94 (d, 2 H, J = 8.3 Hz, Ar), 7.93 (d, 2 H, J = 8.8 Hz, Ar), 7.66 (d, 2 H, J = 8.3 Hz, Ar), 7.55 (d, 2 H, J = 8.8 Hz, Ar), 6.95 (d, 1 H, J = 15.6 Hz, Car-H$_7$'), 6.55–6.6 (m, 5 H, Car), 6.2–6.4 (m, 5 H, Car), 6.1 (m, 3 H, Car), 5.14 (s, 2 H, Im-CH$_2$-Ar), 3.87 (m, 8 H, 4Hex-1-CH$_2$), 3.66 (t, 2 H, J = 7.3 Hz, Im-Hex-1-CH$_2$), 2.47 (s, 6 H, 2Me), 2.32 (s, 6 H, 2Me), 2.0–2.1 (m, 8 H, 4Hex-2-CH$_2$), 2.01 (s, 3 H, Car-Me), 1.94 (s, 3 H, Car-Me), 1.92 (s, 3 H, Car-Me), 1.90 (s, 3 H, Car-Me), 1.8–1.95 (m, 2 H, Car-CH$_2$), 1.63 (s, 3 H, Car-Me), 1.5–1.6 (m, 8 H, 4Hex-3-C*H*$_2$), 1.5 (m, 2 H, Car-CH$_2$), 1.37 (m, 10 H, 4Hex-4-CH$_2$ and Im-Hex-3-CH$_2$), 1.25 (m, 12 H, 4Hex-5-C*H*$_2$, Car-CH$_2$, and Im-Hex-4-CH$_2$), 1.16 (m, 2 H, Im-Hex-5-CH$_2$), 0.94 (s, 6 H, 2Car-Me), 0.9 (m, 15 H, 4Hex-6-Me and Im-Hex-6-Me), –2.5 (br, 2 H, NH). HRMS(FAB): found, m/z 1699.079; calcd for $C_{115}H_{139}N_7O_5$, m/z 1699.092 (M$^+$ + 1).

Acknowledgment. We thank Prof. T. Ohno and Dr. K. Nozaki of Osaka University and Prof. M. Yamamoto and Dr. A. Tsuchida of Kyoto University for the measurement of nanosecond transient absorption spectra. This work was supported by a Grant-in-Aid for Specially Promoted Research (No. 02102005) from the Ministry of Education, Science and Culture of Japan.

Supplementary Material Available: Text and schemes describing additional experimental details (24 pages). Ordering information is given on any current masthead page.